Directional Wavelet Bases Construction on Dyadic Quincunx Lattice

Rujie Yin, Ingrid Daubechies

September 28, 2016

Abstract

We construct directional wavelet systems that will enable building efficient signal representation schemes with good direction selectivity. In particular, we focus on wavelet bases on a dyadic quincunx lattice. In our previous work [9], We show that the supports of orthonormal wavelets in our framework are discontinuous in the frequency domain, yet this irregularity constraint can be avoided in frames, even with redundancy factor less than 2. In this paper, we focus on the construction of bi-orthogonal wavelets and show that the same obstruction of regularity as in orthonormal schemes exists in bi-orthogonal schemes. In addition, we provide a numerical algorithm for bi-orthogonal wavelets construction that reveals its intrinsic irregularity.

1 Introduction

In image compression and analysis, 2D tensor wavelet schemes are widely used. Despite the time-frequency localization inherited from 1D wavelet, 2D tensor wavelets suffer from poor orientation selectivity: only horizontal or vertical edges are well represented by tensor wavelets. To obtain better representation of 2D images, several directional wavelet schemes have been proposed and applied to image processing, such as directional wavelet filterbanks (DFB) and various extensions.

Conventional DFB [1] divides the square frequency domain associated with a regular 2D lattice into eight equi-angular pairs of triangles; such schemes can be critically downsampled (maximally decimated) with perfect reconstruction (PR), but they typically do not have a multi-resolution structure. Different approaches have been proposed to generalize DFB to multi-resolution systems, including non-uniform DFB (nuDFB), contourlets, curvelets, shearlets and dual-tree wavelets. nuDFB is introduced in [2] based on multi-resolution analysis (MRA), where at each level of decomposition the square frequency domain is divided into a high frequency outer ring and a central low frequency domain. For nuDFB, the high frequency ring is primarily divided further into six equi-angular pairs of trapezoids and the central low frequency square is kept intact for division in the next level of decomposition, see Fig. 1. The nuDFB filters are solved by optimization which provides a non-unique near orthogonal or bi-orthogonal solution depending on the initialization. Contourlets [3] combine the Laplacian pyramid scheme with DFB which has PR but with redundancy 4/3 inherited from the Laplacian pyramid. Shearlet [4, 5] and curvelet [6] systems construct a multi-resolution partition of the frequency domain by applying shear or rotation operators to a generator function in each level of frequency decomposition. Available shearlet and curvelet implementations have redundancy at least 4; moreover, the factor may grow with the number of directions in the decomposition level. Dual-tree wavelets [7] are linear combinations of 2D tensor wavelets (corresponding to multi-resolution systems) that constitute an approximate Hilbert transform pair, where the high frequency ring is divided into pairs of squares of different directional preference.

However, none of these multi-resolution schemes is PR, critically downsampled and regularized (localized in both time and frequency). In the framework of nuDFB ([2]), it was shown by Durand [8] that it is impossible to construct orthonormal filters localized in frequency without discontinuity in their frequency support, or – equivalently – regularized filters without aliasing. His construction of directional filters uses compositions of 2-band filters associated to quincunx lattice, similar to that of uniform DFB in [2]; as pointed out in [2] the overall composed filters are not alias-free. It is not clear whether Durand's argument also precludes the existence of a regularized wavelet system, if one slightly weakens the set of conditions.

To study this question, we consider multi-resolution directional wavelets corresponding to the same partition of frequency domain as nuDFB and build a framework to analyze the equivalent conditions of PR for critically downsampled as well as more general redundant schemes. In our previous work [9], we show that in MRA on a dyadic quincunx lattice, PR is equivalent to an identity condition and a set of shift-cancellation conditions closely related to the frequency support of filters and their downsampling scheme. Based on these two conditions, we rederived Durand's discontinuity result of orthonormal schemes; we also show that a slight relaxation of conditions allows frames with redundancy less than 2 that circumvent the regularity limitation. Furthermore, we have an explicit approach to construct such regularized directional wavelet frames by smoothing the Fourier transform of the irregular directional wavelets. The main contribution of this paper is that we extend our previous work and show that the same obstruction to regularity as in orthonormal schemes exists in bi-orthogonal schemes. Different from our previous approach in the orthonormal case, our analysis of bi-orthogonal schemes is inspired by Cohen et al's approach in [10] for numerical construction of compactly supported symmetric wavelet bases on a hexagonal lattice. We extend and adapt their numerical construction to our bi-orthogonal setting.

The paper is organized as follows. In Section 2, we set up the framework of an MRA with dyadic quincunx downsampling. In Section 3, we review the regularity analysis of orthonormal schemes and its extension to frames in [9]. In particular, we derive two conditions, *identity summation* and *shift cancellation*, equivalent to perfect reconstruction in this MRA with critical downsampling. These lead to the classification of *regular/singular* boundaries of the frequency partition and a *relaxed shift-cancellation* condition for low-redundancy MRA frame allows better regularity of the directional wavelets. In Section 4, we extend the orthonormal schemes to bi-orthogonal schemes as well as the corresponding *identity summation* and *shift cancellation* conditions. We then introduce Cohen et al's approach in [10] and adapt it to the regularity analysis on our bi-orthogonal schemes due to these conditions. We show that the bi-orthogonal schemes have the same irregularity as in the orthonormal schemes. In Section 5, we propose a numerical algorithm for the construction of bi-orthogonal schemes along with further analysis on the regularity constraints. Finally, we present numerical results of our algorithm in Section 6, conclude our current work and discuss future work in Section 7.

2 Framework Setup

We summarize 2D-MRA systems and the relation between frequency domain partition and sub-lattice of $\mathbb{Z}^2$ with critical downsampling following [9].

2.1 Notation

Throughout this paper, we use upper case bold font for matrices (*e.g.* $\boldsymbol{A}, \boldsymbol{B}$), lower case bold font for vectors (*e.g.* $\boldsymbol{a}, \boldsymbol{b}$) and upper case italics for subsets (*e.g.* C_1, C_2) of the frequency domain. We denote the conjugate transpose of a matrix $\boldsymbol{A}$ by $\boldsymbol{A}^*$. For $\boldsymbol{a}$ in a d-dimensional vector space over $\mathbb{F}$, we use the convention $\boldsymbol{a} \in \mathbb{F}^{d\times 1}$ and $\boldsymbol{a}^*$ for its conjugate row vector. For matrices and vectors, the indexing of rows and columns starts with zero.

2.2 Multi-resolution analysis and sub-lattice sampling

In an MRA, given a scaling function $\phi \in L^2(\mathbb{R}^2)$, s.t. $\|\phi\|_2 = 1$, the base approximation space is defined as $V_0 = \overline{span\{\phi_{0,\boldsymbol{k}}\}}_{\boldsymbol{k}\in\mathbb{Z}^2}$, where $\phi_{0,\boldsymbol{k}} = \phi(\boldsymbol{x} - \boldsymbol{k})$. If $\langle \phi_{0,\boldsymbol{k}}, \phi_{0,\boldsymbol{k}'}\rangle = \delta_{\boldsymbol{k},\boldsymbol{k}'}$, then $\{\phi_{0,\boldsymbol{k}}\}$ is an orthonormal basis of V_0. In addition, ϕ is associated with a scaling matrix $\mathbf{D} \in \mathbb{Z}^{2\times 2}$, s.t. the dilated scaling function $\phi_1(\boldsymbol{x}) = |\mathbf{D}|^{-1/2}\phi(\mathbf{D}^{-1}\boldsymbol{x})$ is a linear combination of $\phi_{0,\boldsymbol{k}}$. Equivalently, $\exists\, m_0(\boldsymbol{\omega}) = m_0(\omega_1, \omega_2)$, $2\pi-$periodic in ω_1, ω_2, s.t. in the frequency domain

$$\widehat{\phi}(\mathbf{D}^T\boldsymbol{\omega}) = m_0(\boldsymbol{\omega})\widehat{\phi}(\boldsymbol{\omega}). \tag{1}$$

The recursive expression (1) of $\widehat{\phi}(\boldsymbol{\omega})$ implies that

$$\widehat{\phi}(\boldsymbol{\omega}) = (2\pi)^{-1}\prod_{k=1}^{\infty} m_0(\mathbf{D}^{-k}\boldsymbol{\omega}), \tag{2}$$

where we have implicitly assumed that $\phi \in L^1(\mathbb{R}^2)$ and $\int \phi\, dx = 1$ (which follows from the other constraints if ϕ has some decay at ∞).

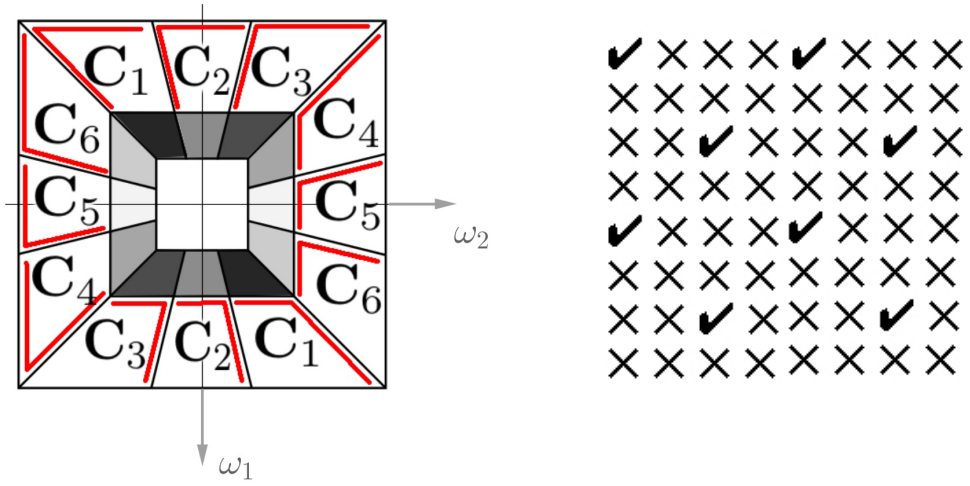

Figure 1: Left: partition of S_0 and boundary assignment of C_j, $j = 1, \cdots, 6$ (each C_j has boundaries indicated by red line segments), Right: dyadic quincunx sub-lattice.

Let $\phi_{l,\boldsymbol{k}} = \phi(\boldsymbol{D}^{-l}\boldsymbol{x} - \boldsymbol{k})$ and $V_l = \overline{span\{\phi_{l,\boldsymbol{k}}; \boldsymbol{k} \in \mathbb{Z}^2\}}$, $l \in \mathbb{Z}$ be the nested approximation spaces. Define W_l as the orthogonal complement of V_l with respect to V_{l-1} in MRA. Suppose there are J wavelet functions $\psi^j \in L^2(\mathbb{R}^2)$, $1 \le j \le J$, and $\mathbf{Q} \in \mathbb{Z}^{2\times 2}$, s.t.

$$W_l = \bigcup_{j=1}^{J} W_l^j = \bigcup_{j=1}^{J} \overline{span\{\psi^j_{l,\boldsymbol{k}}; \boldsymbol{k} \in \mathbf{Q}\mathbb{Z}^2\}} = \bigcup_{j=1}^{J} \overline{span\{\psi^j(\mathbf{D}^{-l}\boldsymbol{x} - \boldsymbol{k}); \boldsymbol{k} \in \mathbf{Q}\mathbb{Z}^2\}},$$

an L-level multi-resolution system with base space V_0 is then spanned by

$$V_L \oplus \bigoplus_{l=1}^{L} \Big(\bigcup_{j=1}^{J} W_l^j \Big) = \{\phi_{L,\boldsymbol{k}}, \psi^j_{l,\boldsymbol{k'}},\ 1 \le l \le L,\ \boldsymbol{k} \in \mathbb{Z}^2,\ \boldsymbol{k'} \in \mathbf{Q}\mathbb{Z}^2,\ 1 \le j \le J\}. \tag{3}$$

In particular, we set $\mathbf{D} = \mathbf{D_2} \doteq \left(\begin{smallmatrix} 2 & 0 \\ 0 & 2 \end{smallmatrix}\right)$ and $\mathbf{Q} \doteq \left(\begin{smallmatrix} 1 & 1 \\ -1 & 1 \end{smallmatrix}\right)$. As $W_1 \subset V_0$, each rescaled wavelet $\psi^j(\mathbf{D}^{-1}\cdot)$ is also a linear combination of $\phi_{0,\boldsymbol{k}}$, so that $\exists\, m_j$ analogous to m_0 satisfying

$$\widehat{\psi^j}(\mathbf{D}^T\boldsymbol{\omega}) = m_j(\boldsymbol{\omega})\widehat{\phi}(\boldsymbol{\omega}), \qquad 1 \le j \le J. \tag{4}$$

In this specific construction of MRA, the corresponding subsampling matrix of $\phi_{1,\boldsymbol{k}}$ is $\mathbf{D}$ and that of $\psi^j_{1,\boldsymbol{k}}$ is $\mathbf{QD}$, the dyadic quincunx subsample (see the right panel in Fig.1), as in [8].

2.3 Frequency domain partition and critical downsampling

Consider the canonical frequency square, $S_0 = [-\pi, \pi) \times [-\pi, \pi)$ associated with the lattice $\mathcal{L} = \mathbb{Z}^2$. For $L = 1$, the 1-level decomposition (3) together with (1) and (4) implies that the union of the support of m_j, $0 \le j \le J$ covers S_0. Furthermore, $\exists\, C_j \subset supp(m_j), 0 \le j \le J$, such that they form a partition of S_0; conversely, given a partition C_j of S_0, we may construct an MRA where m_j are "mainly" supported on C_j (this will become more explicit in Section 4.3). To build an orthonormal basis with good directional selectivity, we choose the partition of S_0 shown in the left of Fig.1, which is the same for Example B in [8] and the least redundant shearlet system [12]. In this partition, S_0 is divided into a central square $C_0 = \left(\begin{smallmatrix} 2 & 0 \\ 0 & 2 \end{smallmatrix}\right)^{-1} S_0$ and a ring: the ring is further cut into six pairs of directional trapezoids C_j by lines passing through the origin with slopes $\pm 1, \pm 3$ and $\pm\frac{1}{3}$. The central square C_0 can be further partitioned in the same way to obtain a two-level multi-resolution system, as shown in Fig.1.

Here $J = 6$ and $|\mathbf{D}|^{-1} + J|\mathbf{QD}|^{-1} = 1/4 + 6/(2 \cdot 4) = 1$, hence the corresponding MRA generated by (3) achieves critical downsampling([8]). In addition, let $\boldsymbol{\pi}_0 = (0,0), \boldsymbol{\pi}_1 = (\pi/2, \pi/2), \boldsymbol{\pi}_2 = (\pi, 0), \boldsymbol{\pi}_3 = (-\pi/2, \pi/2), \boldsymbol{\pi}_4 = (0, \pi), \boldsymbol{\pi}_5 = (\pi/2, -\pi/2), \boldsymbol{\pi}_6 = (\pi, \pi), \boldsymbol{\pi}_7 = (-\pi/2, -\pi/2)$, then each piece C_j together with its shifts form a tiling of S_0, i.e.

$$S_0 = \bigcup_{\boldsymbol{\pi} \in \Gamma_1} (C_j + \boldsymbol{\pi}) = \bigcup_{\boldsymbol{\pi} \in \Gamma_0} (C_0 + \boldsymbol{\pi}), \quad j = 1, \cdots, 6 \tag{5}$$

where $\Gamma_0 = \{\boldsymbol{\pi}_i,\, i = 0, 2, 4, 6\}$ and $\Gamma_1 = \{\boldsymbol{\pi}_i,\, i = 0, 1, \cdots, 7\}$. Alternatively, we say that $\{\, C_j,\, j = 0, \cdots, 6\,\}$ is an *admissible* partition of S_0.

3 Orthonormal Bases

In this section, we discuss the conditions on m_j such that the corresponding MRA forms an orthonormal bases.

We begin with the two key conditions, i.e. *identity summation* and *shift cancellation*, on m_j such that the system (3) is perfect-reconstruction (PR) or equivalently a Parseval frame in MRA.

3.1 orthonormal conditions on m_j

In MRA, (3) is PR if $\forall f \in L_2(\mathbb{R}^2)$,

$$\sum_{\boldsymbol{k}\in\mathbb{Z}^2} \langle f, \phi_{0,\boldsymbol{k}}\rangle \phi_{0,\boldsymbol{k}} = \sum_{\boldsymbol{k}\in\mathbb{Z}^2} \langle f, \phi_{1,\boldsymbol{k}}\rangle \phi_{1,\boldsymbol{k}} + \sum_{j=1}^{J} \sum_{\boldsymbol{k}'\in \boldsymbol{Q}\mathbb{Z}^2} \langle f, \psi^j_{1,\boldsymbol{k}'}\rangle \psi^j_{1,\boldsymbol{k}'}. \tag{6}$$

Using (1) and (4) together with the admissibility of the frequency partition (5), condition (6) on ϕ and ψ^j yields:

Theorem 1. *The perfect reconstruction condition holds for* (3) *iff the following two conditions hold*

$$|m_0(\boldsymbol{\omega})|^2 + \sum_{j=1}^{6} |m_j(\boldsymbol{\omega})|^2 = 1 \tag{7}$$

$$\begin{cases} \sum_{j=0}^{6} m_j(\boldsymbol{\omega})\overline{m_j}(\boldsymbol{\omega}+\boldsymbol{\pi}) = 0, & \boldsymbol{\pi} \in \Gamma_0 \setminus \{\mathbf{0}\} \\ \sum_{j=1}^{6} m_j(\boldsymbol{\omega})\overline{m_j}(\boldsymbol{\omega}+\boldsymbol{\pi}) = 0, & \boldsymbol{\pi} \in \Gamma_1 \setminus \Gamma_0 \end{cases} \tag{8}$$

Theorem 1 is a corollary of Prop. 1 and Prop. 2 in [8]. We give an alternate proof in Appendix A. In Theorem 1, Eq. (7) is the *identity summation* condition, guaranteeing conservation of l_2 energy; Eq. (8) is the *shift cancellation* condition such that aliasing is canceled correctly in reconstruction from wavelet coefficients.

Moreover, for (3) to be an orthonormal basis, $\{\phi_{\boldsymbol{k}}\}_{\boldsymbol{k}\in\mathbb{Z}^2}$ need to be an orthonormal basis, which is determined by m_0 in (2). In 1D MRA, Cohen's theorem in [11] provides a necessary and sufficient condition on m_0 such that (3) is an orthonormal basis. This theorem generalizes to 2D as proved in e.g. [9], as follows.

Theorem 2. *Assume that m_0 is a trigonometric polynomial with $m_0(\mathbf{0}) = 1$, and define $\hat{\phi}(\boldsymbol{\omega})$ as in* (2). *If $\phi(\cdot - \boldsymbol{k}), \boldsymbol{k} \in \mathbb{Z}^2$ are orthonormal, then $\exists K$ containing a neighborhood of 0, s.t. $\forall \boldsymbol{\omega} \in S_0$, $\boldsymbol{\omega} + 2\pi\mathbf{n} \in K$ for some $\mathbf{n} \in \mathbb{Z}^2$, and $\inf_{k>0,\,\boldsymbol{\omega}\in K} |m_0(\mathbf{D_2}^{-k}\boldsymbol{\omega})| > 0$. Further, if $\sum_{\boldsymbol{\pi}\in\Gamma_0} |m_0(\boldsymbol{\omega}+\boldsymbol{\pi})|^2 = 1$, then the inverse is true.*

3.2 Regularity of m_j supported on the C_j

In this subsection, we consider m_j supported on the C_j introduced in Section 2.3 that satisfy orthonormal conditions in Section 3.1. We begin with the Shannon-type wavelet construction, where m_j are indicator functions $m_j = \mathbb{1}_{C_j}$, $0 \le j \le 6$, and we use the boundary assignment of C_j in Fig.1. The identity summation follows from the partition of S_0 by the C_j, and the shift cancellation follows from the tiling property (5). Applying Theorem 2 to m_0, we verify that the Shannon-type wavelets generated from these m_j form an orthonormal basis.

Because of the discontinuity at ∂C_j, the boundaries of the C_j, these m_j are not smooth, and hence the corresponding wavelets are not spatially localized. The m_j can be regularized by smoothing at the ∂C_j. However, as shown in Proposition 3 in [8], it is not possible to smooth the behavior of the m_j at *all* the boundaries with discontinuity if the m_j have to satisfy the perfect reconstruction condition. In [9], the ∂C_j are segmented into *singular* and *regular* pieces. On regular boundaries, pairs of $(m_j,\, m_{j'})$ share a boundary and can both be smoothed in a coherent way such that all the constraints in Theorem 2 remain satisfied.

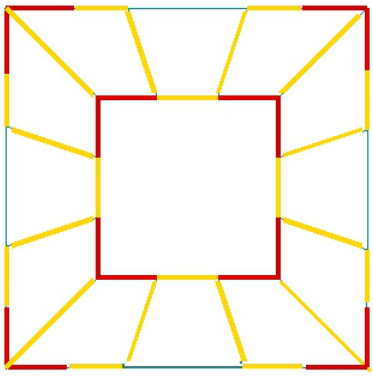

Figure 2: Boundary classification, singular (red) and regular (yellow)

The singular pieces are boundaries for just one m_j, which can then not be smoothed without violating the shift cancellation condition. Fig. 2 shows the boundary classification, where the corners of S_0 and C_0 are singular, hence m_0 and the m_j's in two diagonal directions of an orthonormal bases are discontinuous there. A mechanism of constructing orthonormal bases by smoothing Shannon-type m_j on regular boundaries is provided in [9].

3.3 Extension to low-redundancy tight frame

The irregularity of orthonormal bases can be overcome in the following low-redundancy tight frame construction,

$$\{\phi_{L,\boldsymbol{k}}\,, \psi^j_{l,\boldsymbol{k'}}\,,\ 1 \le l \le L,\ \boldsymbol{k},\ \boldsymbol{k'} \in \mathbb{Z}^2,\ 1 \le j \le J\}. \tag{9}$$

All wavelet coefficients are sub-sampled on dyadic sub-lattice and the redundancy of any $L-$level MRA frame doesn't exceed $\frac{J/|D|}{1-1/|D|} = \frac{6/4}{1-1/4} = 2$. Similar to Theorem 1, we have

Theorem 3. *The perfect reconstruction condition holds for* (9) *iff the following both hold*

$$|m_0(\boldsymbol{\omega})|^2 + \textstyle\sum_{j=1}^{6} |m_j(\boldsymbol{\omega})|^2 = 1 \tag{10}$$

$$\textstyle\sum_{j=0}^{6}\ m_j(\boldsymbol{\omega})\overline{m_j}(\boldsymbol{\omega}+\boldsymbol{\pi}) = 0, \quad \boldsymbol{\pi} \in \Gamma_0 \setminus \{\mathbf{0}\} \tag{11}$$

Theorem 3 can be proved analogously to Theorem 1, but with fewer shift cancellation constraints. Following the same analysis of boundary regularity as before, we show in [9] that all boundaries are regular and can be smoothed properly. Hence, we were able to obtain directional wavelets with much better spatial and frequency localization than those constructed by Durand in [8].

So far, we have considered two directional wavelet MRA systems (3) and (9) such that the directional wavelets characterize 2D signals in six equi-angled directions. Furthermore, these wavelets are well localized in the frequency domain such that $supp(m_j)$ is convex and $\exists\, \epsilon\ s.t.$

$$\sup_{\boldsymbol{\omega'} \in supp(m_j)}\ \inf_{\boldsymbol{\omega} \in C_j} \|\boldsymbol{\omega'} - \boldsymbol{\omega}\| < \epsilon, \quad 0 \le j \le 6. \tag{12}$$

This desirable condition is hard to obtain by multi-directional filter bank assembly of several elementary filter banks.

In the next section, we analyze the more general case of directional bi-orthorgonal filters constructed with respect to the same frequency partition.

4 Bi-orthogonal Bases

In this section, we analyze bi-orthogonal bases in the following form of MRA,

$$\{\phi_{L,\boldsymbol{k}}, \widetilde{\phi}_{L,\boldsymbol{k}}, \psi^j_{l,\boldsymbol{k'}}, \widetilde{\psi}^j_{l,\boldsymbol{k'}},\ 1 \le l \le L,\ \boldsymbol{k} \in \mathbb{Z}^2,\ \boldsymbol{k'} \in \mathbf{Q}\mathbb{Z}^2,\ 1 \le j \le J\}, \tag{13}$$

where ϕ and ψ^j satisfy (1) and (4), as well as $\widetilde{\phi}$ and $\widetilde{\psi^j}$, respectively,

$$\widehat{\widetilde{\phi}}(\boldsymbol{D}^T\boldsymbol{\omega}) = \widetilde{m_0}(\boldsymbol{\omega})\widehat{\widetilde{\phi}}(\boldsymbol{\omega}), \quad \widehat{\widetilde{\psi^j}}(\boldsymbol{D}^T\boldsymbol{\omega}) = \widetilde{m_j}(\boldsymbol{\omega})\widehat{\widetilde{\phi}}(\boldsymbol{\omega}). \tag{14}$$

For such bi-orthogonal bases, we have the similar identity summation and shift cancellation conditions to those in Theorem 1.

Theorem 4. *The perfect reconstruction iff the following two conditions hold*

$$m_0(\boldsymbol{\omega})\overline{\widetilde{m_0}}(\boldsymbol{\omega}) + \sum_{j=1}^{6} m_j(\boldsymbol{\omega})\overline{\widetilde{m_j}}(\boldsymbol{\omega}) = 1 \tag{15}$$

$$\begin{cases} \sum_{j=0}^{6} m_j(\boldsymbol{\omega})\overline{\widetilde{m_j}}(\boldsymbol{\omega}+\boldsymbol{\pi}) = 0, & \boldsymbol{\pi} \in \Gamma_0 \setminus \{\mathbf{0}\} \\ \sum_{j=1}^{6} m_j(\boldsymbol{\omega})\overline{\widetilde{m_j}}(\boldsymbol{\omega}+\boldsymbol{\pi}) = 0, & \boldsymbol{\pi} \in \Gamma_1 \setminus \Gamma_0 \end{cases} \tag{16}$$

We also have the following analogue of Theorem 2.

Theorem 5. *Assume that $m_0, \widetilde{m_0}$ are trigonometric polynomials with $m_0(\mathbf{0}) = \widetilde{m_0}(\mathbf{0}) = 1$, which generate $\phi, \widetilde{\phi}$ respectively.*
If $\phi(\cdot-\boldsymbol{k}), \widetilde{\phi}(\cdot-\boldsymbol{k})$, $\boldsymbol{k} \in \mathbb{Z}^2$ are bi-orthogonal, then $\exists K$ containing a neighborhood of 0, s.t. $\forall \boldsymbol{\omega} \in S_0$, $\boldsymbol{\omega}+2\pi\mathbf{n} \in K$ for some $\mathbf{n} \in \mathbb{Z}^2$, and $\inf_{k>0,\,\boldsymbol{\omega}\in K} |m_0(\mathbf{D_2}^{-k}\boldsymbol{\omega})| > 0$, $\inf_{k>0,\,\boldsymbol{\omega}\in K} |\widetilde{m_0}(\mathbf{D_2}^{-k}\boldsymbol{\omega})| > 0$. Furthermore, if $\sum_{\boldsymbol{\pi}\in\Gamma_0} m_0(\boldsymbol{\omega}+\boldsymbol{\pi})\overline{\widetilde{m_0}}(\boldsymbol{\omega}+\boldsymbol{\pi}) = 1$, then the inverse is true.

By Theorem 5, m_0 and $\widetilde{m_0}$ need to satisfy the following identity constraint for the MRA (13) to be bi-orthogonal,

$$m_0\overline{\widetilde{m_0}}(\boldsymbol{\omega}) + m_0\overline{\widetilde{m_0}}(\boldsymbol{\omega}+\boldsymbol{\pi}_2) + m_0\overline{\widetilde{m_0}}(\boldsymbol{\omega}+\boldsymbol{\pi}_4) + m_0\overline{\widetilde{m_0}}(\boldsymbol{\omega}+\boldsymbol{\pi}_6) = 1. \tag{17}$$

In addition, the identity summation and shift cancellation conditions (15) and (16) from Theorem 4 can be combined into a linear system with respect to m_j as follows,

$$\begin{bmatrix} \overline{\widetilde{m_0}}(\boldsymbol{\omega}) & \overline{\widetilde{m_1}}(\boldsymbol{\omega}) & \dots & \overline{\widetilde{m_6}}(\boldsymbol{\omega}) \\ 0 & \overline{\widetilde{m_1}}(\boldsymbol{\omega}+\boldsymbol{\pi}_1) & \dots & \overline{\widetilde{m_6}}(\boldsymbol{\omega}+\boldsymbol{\pi}_1) \\ \overline{\widetilde{m_0}}(\boldsymbol{\omega}+\boldsymbol{\pi}_2) & \overline{\widetilde{m_1}}(\boldsymbol{\omega}+\boldsymbol{\pi}_2) & \dots & \overline{\widetilde{m_6}}(\boldsymbol{\omega}+\boldsymbol{\pi}_2) \\ \vdots & \vdots & \vdots & \vdots \\ 0 & \overline{\widetilde{m_1}}(\boldsymbol{\omega}+\boldsymbol{\pi}_7) & \dots & \overline{\widetilde{m_6}}(\boldsymbol{\omega}+\boldsymbol{\pi}_7) \end{bmatrix} \begin{bmatrix} m_0(\boldsymbol{\omega}) \\ m_1(\boldsymbol{\omega}) \\ m_2(\boldsymbol{\omega}) \\ \vdots \\ m_6(\boldsymbol{\omega}) \end{bmatrix} = \begin{bmatrix} 1 \\ 0 \\ 0 \\ \vdots \\ 0 \end{bmatrix} \tag{18}$$

In sum, the construction of a bi-orthogonal basis (13) is equivalent to find feasible solutions of (18) with constraint (17)[1]. To solve this, we use the same approach as in [10], which constructs compactly supported symmetric bi-orthogonal filters on a hexagon lattice. We next review the main scheme in [10] and adapt it to our setup of bi-orthogonal bases on the dyadic quincunx lattice.

4.1 Summary of Cohen et al's construction

We summerize the main setup and the approach in [10]. Consider a bi-orthogonal scheme consists of three high-pass filters m_1, m_2 and m_3 and a low-pass filter m_0 together with their bi-orthogonal duals $\widetilde{m_j}$, s.t. m_0 and $\widetilde{m_0}$ are $\frac{2\pi}{3}$-rotation invariant and m_1, m_2, m_3 and their duals are $\frac{2\pi}{3}$-rotation co-variant on a hexagon lattice.

This bi-orthogonal scheme satisfies the following linear system (Lemma 2.2.2 in [10])

$$\begin{bmatrix} \overline{\widetilde{m_0}}(\boldsymbol{\omega}) & \overline{\widetilde{m_1}}(\boldsymbol{\omega}) & \overline{\widetilde{m_2}}(\boldsymbol{\omega}) & \overline{\widetilde{m_3}}(\boldsymbol{\omega}) \\ \overline{\widetilde{m_0}}(\boldsymbol{\omega}+\boldsymbol{\nu}_1) & \overline{\widetilde{m_1}}(\boldsymbol{\omega}+\boldsymbol{\nu}_1) & \overline{\widetilde{m_2}}(\boldsymbol{\omega}+\boldsymbol{\nu}_1) & \overline{\widetilde{m_3}}(\boldsymbol{\omega}+\boldsymbol{\nu}_1) \\ \overline{\widetilde{m_0}}(\boldsymbol{\omega}+\boldsymbol{\nu}_2) & \overline{\widetilde{m_1}}(\boldsymbol{\omega}+\boldsymbol{\nu}_2) & \overline{\widetilde{m_2}}(\boldsymbol{\omega}+\boldsymbol{\nu}_2) & \overline{\widetilde{m_3}}(\boldsymbol{\omega}+\boldsymbol{\nu}_2) \\ \overline{\widetilde{m_0}}(\boldsymbol{\omega}+\boldsymbol{\nu}_3) & \overline{\widetilde{m_1}}(\boldsymbol{\omega}+\boldsymbol{\nu}_3) & \overline{\widetilde{m_2}}(\boldsymbol{\omega}+\boldsymbol{\nu}_3) & \overline{\widetilde{m_3}}(\boldsymbol{\omega}+\boldsymbol{\nu}_3) \end{bmatrix} \begin{bmatrix} m_0(\boldsymbol{\omega}) \\ m_1(\boldsymbol{\omega}) \\ m_2(\boldsymbol{\omega}) \\ m_3(\boldsymbol{\omega}) \end{bmatrix} = \begin{bmatrix} 1 \\ 0 \\ 0 \\ 0 \end{bmatrix} \tag{19}$$

[1]It can be shown that as long as (18) has a unique solution for m_j given fixed $\widetilde{m_j}$, $j = 0, \cdots, 6$, (17) always holds. See Section 4.2.

where $\boldsymbol{\nu}_i = \boldsymbol{\pi}_{2i}$, $i = 1, 2, 3$. Let $\widetilde{\mathbf{M}}(\boldsymbol{\omega}) \in \mathbb{C}^{4\times 4}$ be the matrix with entries $\overline{\widetilde{m_j}}(\boldsymbol{\omega} + \boldsymbol{\nu}_i)$ and $\mathbf{m}(\boldsymbol{\omega}) \in \mathbb{C}^4$ be the vector consisting of entries $m_j(\boldsymbol{\omega})$ in (19), then (19) can be written as

$$\widetilde{\mathbf{M}}(\boldsymbol{\omega})\,\mathbf{m}(\boldsymbol{\omega}) = [1, 0, 0, 0]^\top.$$

Begin with a pre-designed $\widetilde{m_1}(\boldsymbol{\omega})$ with desired propery, $\widetilde{m_2}(\boldsymbol{\omega})$ and $\widetilde{m_3}(\boldsymbol{\omega})$ are determined by symmetry. Lemma 2.2.2 in [10] then leads to

$$\begin{aligned} m_0(\boldsymbol{\omega}) &= D^{-1} \begin{vmatrix} \overline{\widetilde{m_1}}(\boldsymbol{\omega}+\boldsymbol{\nu}_1) & \overline{\widetilde{m_2}}(\boldsymbol{\omega}+\boldsymbol{\nu}_1) & \overline{\widetilde{m_3}}(\boldsymbol{\omega}+\boldsymbol{\nu}_1) \\ \overline{\widetilde{m_1}}(\boldsymbol{\omega}+\boldsymbol{\nu}_2) & \overline{\widetilde{m_2}}(\boldsymbol{\omega}+\boldsymbol{\nu}_2) & \overline{\widetilde{m_3}}(\boldsymbol{\omega}+\boldsymbol{\nu}_2) \\ \overline{\widetilde{m_1}}(\boldsymbol{\omega}+\boldsymbol{\nu}_3) & \overline{\widetilde{m_2}}(\boldsymbol{\omega}+\boldsymbol{\nu}_3) & \overline{\widetilde{m_3}}(\boldsymbol{\omega}+\boldsymbol{\nu}_3) \end{vmatrix} \\ &= D^{-1}\widetilde{\mathbf{M}}_{0,0}(\boldsymbol{\omega}), \end{aligned} \tag{20}$$

where $\widetilde{\mathbf{M}}_{0,0}(\boldsymbol{\omega})$ is the minor of $\widetilde{\mathbf{M}}(\boldsymbol{\omega})$ with respect to $\overline{\widetilde{m_0}}(\boldsymbol{\omega})$ and $D \equiv \det(\widetilde{\mathbf{M}}(\boldsymbol{\omega})) \in \mathbb{C}^* = \mathbb{C} \setminus \{0\}$ does not depend on $\boldsymbol{\omega}$ in [10], due to symmetry.

Expanding $det(\widetilde{\mathbf{M}}(\boldsymbol{\omega}))$ with respect to the first column leads to the following constraint on $\widetilde{m_0}(\boldsymbol{\omega})$,

$$m_0\overline{\widetilde{m_0}}(\boldsymbol{\omega}) + m_0\overline{\widetilde{m_0}}(\boldsymbol{\omega}+\boldsymbol{\nu}_1) + m_0\overline{\widetilde{m_0}}(\boldsymbol{\omega}+\boldsymbol{\nu}_2) + m_0\overline{\widetilde{m_0}}(\boldsymbol{\omega}+\boldsymbol{\nu}_3) = 1, \tag{21}$$

which is the same as the identity constraint (17) for bi-orthogonal bases. Once (21) is solved for $\widetilde{m_0}$, m_1, m_2 and m_3 are obtained by solving the linear system (19) with known $\widetilde{\mathbf{M}}(\boldsymbol{\omega})$.

4.2 Adaptation to dyadic quincunx downsampling

Despite the specific symmetries of m_j, $\widetilde{m_j}$, $j = 0, \cdots, 3$ on a hexagon lattice, Cohen et al's approach can be adapted to construct bi-orthogonal bases on different lattices with different downsampling schemes. In particular, we adapt their approach to solve (18) where $\widetilde{m_j}$, $j = 1, \cdots, 6$ are pre-designed. Furthermore, by exploiting the symmetric structure of (18) with respect to the shifts $\boldsymbol{\pi}_i$, $i = 0, \cdots, 7$, we derive necessary conditions for (18) to have a unique solution which imply the irregularity in our bi-orthogonal scheme.

Since (18) takes the same form as (19), for simplicity, in the rest of this paper, we adapt the matrix and vector notations $\widetilde{\mathbf{M}}(\boldsymbol{\omega})$, $\mathbf{m}(\boldsymbol{\omega})$ that helped to simplify (19). Accordingly, we rewrite (18) as

$$\widetilde{\mathbf{M}}(\boldsymbol{\omega})\,\mathbf{m}(\boldsymbol{\omega}) = [1, 0, 0, 0, 0, 0, 0, 0]^\top,$$

where $\widetilde{\mathbf{M}}(\boldsymbol{\omega}) \in \mathbb{C}^{8\times 7}$ and $\mathbf{m}(\boldsymbol{\omega}) \in \mathbb{C}^7$. In addition, let $\boldsymbol{b}_k \in \mathbb{R}^8$, $0 \le k \le 7$, whose only non-zero entry is $\boldsymbol{b}_k[k] = 1$, where the indexing starts with zero. Note that $\widetilde{\mathbf{M}}(\boldsymbol{\omega})\,\mathbf{m}(\boldsymbol{\omega}) = \boldsymbol{b}_0 \in \mathbb{R}^8$ is over-determined; it has a unique solution of m_j if and only if

(5.i) $\widetilde{\mathbf{M}}(\boldsymbol{\omega})$ is full rank,

(5.ii) $[\widetilde{\mathbf{M}}(\boldsymbol{\omega}), \boldsymbol{b}_0]$ is singular,

where we use [ ] to concatenate $\widetilde{\mathbf{M}}(\boldsymbol{\omega})$ and $\boldsymbol{b}_0$ into a 8×8 matrix. The matrix $\widetilde{\mathbf{M}}(\boldsymbol{\omega})$ is structured such that each row is associated with a shift $\boldsymbol{\pi}_i$, $i = 0 \cdots, 7$ and each column is associated with a dual function $\widetilde{m_j}(\boldsymbol{\omega})$, $j = 0, \cdots, 7$. In particular, $\widetilde{\mathbf{M}}(\boldsymbol{\omega})$ depends on the value of $\widetilde{m_j}$ at $\boldsymbol{\omega}$ and its shifts $\boldsymbol{\omega} + \boldsymbol{\pi}_i$, thus can be considered a vector function of $\boldsymbol{\omega}$. We denote a sub-matrix of $\widetilde{\mathbf{M}}$ containing all but the row associated with $\boldsymbol{\pi}_k$ (respectively, the column associated with $\widetilde{m_k}(\boldsymbol{\omega})$) as $\widetilde{\mathbf{M}}[-k, :]$ (respectively, $\widetilde{\mathbf{M}}[:, -k]$). In particular, we denote $\widetilde{\mathbf{M}}[-0, -0]$ as $\widetilde{\mathbf{M}}^{\square}$.

We have the following observations for $\widetilde{\mathbf{M}}(\boldsymbol{\omega})$.

Lemma 4.1. *$\forall \boldsymbol{\omega} \in S_0$, if (18) is solvable, then $\widetilde{\mathbf{M}}[-0, :](\boldsymbol{\omega})$ is singular.*

Proof. If (18) is solvable, then condition (5.ii) holds, which implies that $\det([\widetilde{\mathbf{M}}(\boldsymbol{\omega}), \boldsymbol{b}_0]) = 0$. Expanding the determinant with respect to the last column $\boldsymbol{b}_0$ yields $\det(\,\widetilde{\mathbf{M}}[-0, :](\boldsymbol{\omega})\,) = 0$. □

Lemma 4.2. *$\widetilde{\mathbf{M}}(\boldsymbol{\omega})$, $\widetilde{\mathbf{M}}(\boldsymbol{\omega} + \boldsymbol{\pi}_2)$, $\widetilde{\mathbf{M}}(\boldsymbol{\omega} + \boldsymbol{\pi}_4)$ and $\widetilde{\mathbf{M}}(\boldsymbol{\omega} + \boldsymbol{\pi}_6)$ are the same up to row permutations.* (18) *holds $\forall\, \boldsymbol{\omega}$ if and only if*

$$\widetilde{\mathbf{M}}(\boldsymbol{\omega})\big[\,\mathbf{m}(\boldsymbol{\omega}), \mathbf{m}(\boldsymbol{\omega} + \boldsymbol{\pi}_2), \mathbf{m}(\boldsymbol{\omega} + \boldsymbol{\pi}_4), \mathbf{m}(\boldsymbol{\omega} + \boldsymbol{\pi}_6)\,\big] = \big[\,\boldsymbol{b}_0, \boldsymbol{b}_2, \boldsymbol{b}_4, \boldsymbol{b}_6\,\big].$$

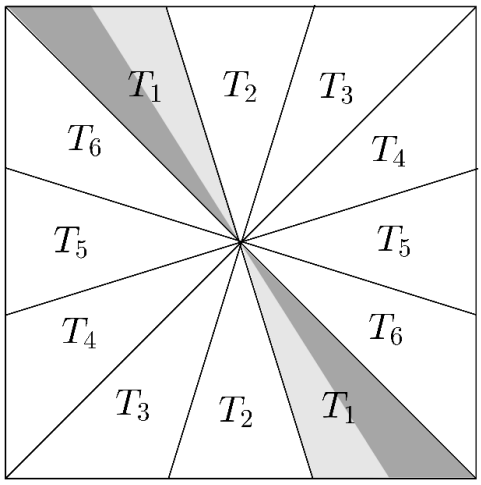

Figure 3: Partition of frequency square in six directions, where the essential support of $\widetilde{m_i}(\boldsymbol{\omega})$ is contained in each pair of triangles T_i. The pair of dark grey triangles is T_1^- and the light grey pair is T_1^+.

Remark. If we consider $\widetilde{\mathbf{M}}(\boldsymbol{\omega})$ a vector function of $\boldsymbol{\omega}$, then the conditions (5.i) and (5.ii) are both pointwise, yet Lemma 4.2 shows that the set of points $\{\boldsymbol{\omega}, \boldsymbol{\omega}+\boldsymbol{\pi}_2, \boldsymbol{\omega}+\boldsymbol{\pi}_4, \boldsymbol{\omega}+\boldsymbol{\pi}_6\}$ are linked together by the symmetry in $\widetilde{\mathbf{M}}(\boldsymbol{\omega})$.

Due to condition (5.i), $\forall\, \boldsymbol{\omega}$, $\exists\, k_{\boldsymbol{\omega}}$ depending on $\boldsymbol{\omega}$ such that $\widetilde{\mathbf{M}}[-k_{\boldsymbol{\omega}}, :](\boldsymbol{\omega})$ is non-singular. Lemma 4.1 implies that $k_{\boldsymbol{\omega}} \neq 0$ [2] ; therefore we may apply Cramer's rule to $\widetilde{\mathbf{M}}[-k_{\boldsymbol{\omega}}, :](\boldsymbol{\omega})$, as in Section 4.1, and obtain the following expression of $m_0(\boldsymbol{\omega})$

$$m_0(\boldsymbol{\omega}) = \det(\,\widetilde{\mathbf{M}}^{\square}[-k_{\boldsymbol{\omega}}, :](\boldsymbol{\omega})\,)/\det(\,\widetilde{\mathbf{M}}[-k_{\boldsymbol{\omega}}, :](\boldsymbol{\omega})\,). \tag{22}$$

Moreover, based on (22), the identity condition (17) on $m_0(\boldsymbol{\omega})$ and $\widetilde{m_0}(\boldsymbol{\omega})$ can be derived in the same way as (21) by expanding $\det(\,\widetilde{\mathbf{M}}[-k_{\boldsymbol{\omega}}, :](\boldsymbol{\omega})\,)$.

4.3 Discontinuity of $\widetilde{m_j}(\boldsymbol{\omega})$

In this subsection, we show our main result that for (18) to be solvable, the pre-designed $\widetilde{m_j}$ are discontinuous, when they satisfy mild conditions on symmetry and concentration of support.

We assume that $|\widetilde{m_1}(\boldsymbol{\omega})|$ and $|\widetilde{m_6}(\boldsymbol{\omega})|$ are symmetric with respect to the diagonal $\omega_1 = \omega_2$, i.e.

$$|\widetilde{m_1}(\boldsymbol{\omega})| = |\widetilde{m_6}(\boldsymbol{\omega}')| \quad \forall\, \omega_1 = \omega_2',\, \omega_2 = \omega_1', \tag{23}$$

and likewise for $\widetilde{m_3}(\boldsymbol{\omega})$ and $\widetilde{m_4}(\boldsymbol{\omega})$,

$$|\widetilde{m_3}(\boldsymbol{\omega})| = |\widetilde{m_4}(\boldsymbol{\omega}')| \quad \forall\, \omega_1 = -\omega_2',\, \omega_2 = -\omega_1'. \tag{24}$$

In the following, we introduce a triangular partition of frequency square and define formally the concentration of $\widetilde{m_j}$'s support.

Definition. The *essential support* Ω_j of a function $\widetilde{m_j}$ is the set $\{\boldsymbol{\omega} : |\widetilde{m_j}(\boldsymbol{\omega})| > |\widetilde{m_i}(\boldsymbol{\omega})|,\, \forall i \neq j\}$.

Let T_j be pairs of triangles shown in Figure 3, such that $C_j \subset T_j$, $j = 1, \cdots, 6$. Consider its decomposition, $T_j = T_j^- \bigcup T_j^+$, where T_j^-, T_j^+ are halves of T_j adjacent to T_{j-1} and T_{j+1} respectively.

Definition. $\widetilde{m_j}$ *concentrates* within T_j if

(i) $\Omega_j \subset T_j$;

(ii) $\mathrm{supp}(\widetilde{m_j}) \subset T_{j-1}^+ \bigcup T_j \bigcup T_{j+1}^-$ and $\int_{\Omega} |\widetilde{m_j}| > \int_{\Omega'} |\widetilde{m_j}|, \forall\, \Omega \subset T_j \bigcap \mathrm{supp}(\widetilde{m_j})$ s.t. $|\Omega| > 0$, where $\Omega' \subset T_{j-1}^+ \bigcup T_{j+1}^-$ is symmetric to Ω with respect to the boundary of T_j.

[2] We have stronger result using the symmetry. Lemma 4.1 and Lemma 4.2 together imply that $\widetilde{\mathbf{M}}[-k, :](\boldsymbol{\omega})$, $k = 0, 2, 4, 6$ are singular. Therefore, $k_{\boldsymbol{\omega}} \in \{1, 3, 5, 7\}$ and thus $\widetilde{\mathbf{M}}[-k_{\boldsymbol{\omega}}, :](\boldsymbol{\omega})$ contains all rows associated with shifts $\boldsymbol{\pi}_{2i}$, $i = 0, \cdots, 3$.

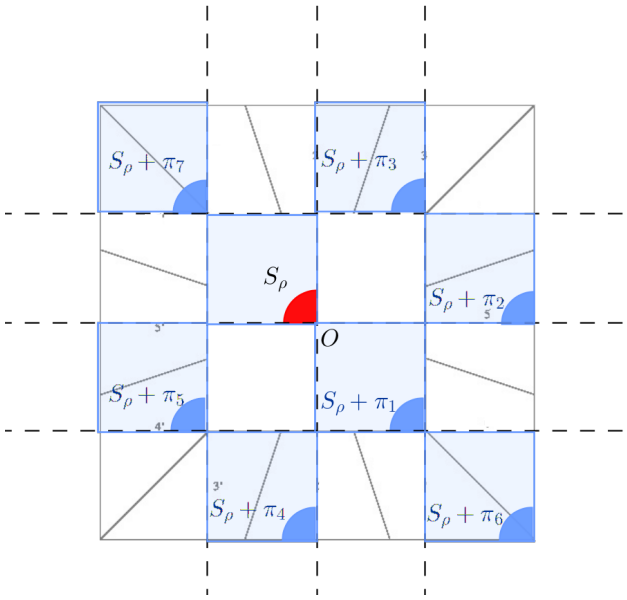

Figure 4: S_ρ and its shifts

Remark. For $\widetilde{m_j}$ to concentrate in T_j, $\widetilde{m_j}$ should be "mainly" supported in T_j (condition (i)) and "decay" properly outside of T_j (conditoin (ii)).

Given $\widetilde{m_j}(\boldsymbol{\omega})$ that concentrates in T_j, we study the singularity condition on $\widetilde{\mathbf{M}}[-0,:](\boldsymbol{\omega})$ from Lemma 4.1, specifically in the domain $S_\rho = \{(\omega_1,\omega_2)|\ \|\omega\| < \rho, \omega_1 < 0,\ \omega_2 < 0\}$, see Figure 4.

Let $\widetilde{\mathbf{m}}^i(\boldsymbol{\omega}) = [\widetilde{m_1}(\boldsymbol{\omega}+\boldsymbol{\pi}_i)\ \cdots,\ \widetilde{m_6}(\boldsymbol{\omega}+\boldsymbol{\pi}_i)] \in \mathbb{C}^6$, $i = 0, \cdots, 7$ be the rows of $\widetilde{\mathbf{M}}[:,-0](\boldsymbol{\omega})$.

Lemma 4.3. *$\exists \rho > 0$ s.t. $\forall \boldsymbol{\omega} \in S_\rho$, if $\widetilde{\mathbf{M}}[-0,:](\boldsymbol{\omega})$ is singular, then $rank(\widetilde{\mathbf{m}}^1(\boldsymbol{\omega}), \widetilde{\mathbf{m}}^7(\boldsymbol{\omega})) = 1$ or $rank(\widetilde{\mathbf{m}}^3(\boldsymbol{\omega}), \widetilde{\mathbf{m}}^5(\boldsymbol{\omega})) = 1$.*

Lemma 4.3 can be proved by analyzing the linear dependency and independency between $\widetilde{\mathbf{m}}^i$ on S_ρ, since $\widetilde{\mathbf{m}}^i$ have known locations of zero entries when ρ is small due to the concentration of $\widetilde{m_j}$. For the full proof of Lemma 4.3, see Appendix B.

The concentration and the symmetry of $\widetilde{m_3}(\boldsymbol{\omega})$ and $\widetilde{m_4}(\boldsymbol{\omega})$ in T_3 and T_4 together imply that $rank(\widetilde{\mathbf{m}}^3, \widetilde{\mathbf{m}}^5) \neq 1$ *a.e.* on S_ρ, see Lemma B.3 in Appendix B.1, hence $rank(\widetilde{\mathbf{m}}^1(\boldsymbol{\omega}), \widetilde{\mathbf{m}}^7(\boldsymbol{\omega})) = 1$ *a.e.* on S_ρ. Therefore, $\widetilde{m_1}(\boldsymbol{\omega}+\boldsymbol{\pi}_1), \widetilde{m_6}(\boldsymbol{\omega}+\boldsymbol{\pi}_1)$ in $\widetilde{\mathbf{m}}^1(\boldsymbol{\omega})$ and the corresponding $\widetilde{m_1}(\boldsymbol{\omega}+\boldsymbol{\pi}_7), \widetilde{m_6}(\boldsymbol{\omega}+\boldsymbol{\pi}_7)$ in $\widetilde{\mathbf{m}}^7(\boldsymbol{\omega})$ on S_ρ are linearly related. Based on this and the concentration and the symmetry of $\widetilde{m_1}(\boldsymbol{\omega})$ and $\widetilde{m_6}(\boldsymbol{\omega})$ in T_1 and T_6, we can show that $\widetilde{m_1}(\boldsymbol{\omega}) = \widetilde{m_6}(\boldsymbol{\omega}) = 0$ *a.e.* on $S_\rho + \boldsymbol{\pi}_1$, see Proposition B.5 in Appendix B.1, which implies the discontinuity of $\widetilde{m_1}(\boldsymbol{\omega})$ and $\widetilde{m_6}(\boldsymbol{\omega})$ at $(\frac{\pi}{2}, \frac{\pi}{2})$ or $(-\frac{\pi}{2}, -\frac{\pi}{2})$.

Proposition 4.4. *Given the same condition as in Lemma 4.3, $\widetilde{m_1}(\boldsymbol{\omega}), \widetilde{m_6}(\boldsymbol{\omega})$ are not continuous at both $(\frac{\pi}{2}, \frac{\pi}{2})$ and $(-\frac{\pi}{2}, -\frac{\pi}{2})$.*

Proof. If $\widetilde{m_1}(\boldsymbol{\omega})$ is continuous at $(\frac{\pi}{2}, \frac{\pi}{2})$, then $\widetilde{m_1}(\frac{\pi}{2}, \frac{\pi}{2}) = \lim_{\alpha \to 1^-} \widetilde{m_1}(\boldsymbol{\omega}(\alpha)) = 0$, where $\{\boldsymbol{\omega}(\alpha), 0 \leq \alpha < 1\} \subset S_\rho + \boldsymbol{\pi}_1$ and $\boldsymbol{\omega}(1) = (\frac{\pi}{2}, \frac{\pi}{2})$. By symmetry, we have $\widetilde{m_6}(\frac{\pi}{2}, \frac{\pi}{2}) = 0$. Similarly, the continuity at $(-\frac{\pi}{2}, -\frac{\pi}{2})$ implies $\widetilde{m_1}(-\frac{\pi}{2}, -\frac{\pi}{2}) = \widetilde{m_6}(-\frac{\pi}{2}, -\frac{\pi}{2}) = 0$. Therefore $\widetilde{\mathbf{m}}^1(\mathbf{0}) = \widetilde{\mathbf{m}}^7(\mathbf{0}) = \mathbf{0}$ at the origin which results in contradiction with Lemma 4.3. □

The following theorem summarizes our main result.

Theorem 4.5. *If $\widetilde{m_j}(\boldsymbol{\omega})$ concentrates in T_j and have symmetries (23) and (24), then (18) doesn't have feasible solution of m_j given continuous $\widetilde{m_1}(\boldsymbol{\omega})$ and $\widetilde{m_6}(\boldsymbol{\omega})$.*

5 Numerical construction of bi-orthogonal bases

In this section, we develop a numerical construction of bi-orthogonal bases on a dyadic quincunx lattice in our previous setup. Following the same approach of Cohen et al, we first design $\widetilde{m_j}(\boldsymbol{\omega})$, $j = 1, \cdots, 6$, on the canonical frequency square $S_0 = [-\pi, \pi) \times [-\pi, \pi)$, then solve for $m_0, \widetilde{m_0}$ and m_j on S_0 in order with respect to (18) and (17).

5.1 Design of input $\widetilde{m_j}(\boldsymbol{\omega})$

In this sub-section, we construct $\widetilde{m_j}(\boldsymbol{\omega})$, $j = 1, \cdots, 6$, which concentrate in T_i. Specifically, following the orthonormal construction in [9], we consider $\widetilde{m_j}(\boldsymbol{\omega})$ in the form

$$\widetilde{m_j}(\boldsymbol{\omega}) = e^{-i\boldsymbol{\eta}_j^\top \boldsymbol{\omega}} |\widetilde{m_j}(\boldsymbol{\omega})|, \quad j = 1, \cdots, 6, \tag{25}$$

where $\boldsymbol{\eta}_j \in \mathbb{Z}^2$ is the phase constant of $\widetilde{m_j}$. In addition to the symmetry of pairs $(|\widetilde{m_1}|, |\widetilde{m_6}|)$ and $(|\widetilde{m_3}|, |\widetilde{m_4}|)$ assumed in Section 4.3, we further request that $|\widetilde{m_2}|$ and $|\widetilde{m_5}|$ are symmetric with respect to the ω_1-axis and ω_2-axis accordingly. Figure 5 shows such a design of $|\widetilde{m_j}(\boldsymbol{\omega})|$ that has the imposed strong symmetries.

Based on (25) and the symmetries of $|\widetilde{m_j}(\boldsymbol{\omega})|$, for $|m_0(\boldsymbol{\omega})| > 0$, $\forall\, |\boldsymbol{\omega}| < \rho$, $\boldsymbol{\eta}_j$ have to satisfy certain constraints.

Lemma 5.1. *If* $\exists\, \boldsymbol{\omega} \in D_1 := \{\omega_1 = \omega_2, \omega_1 \in (-\frac{\pi}{2}, 0)\}$, *s.t.* $|m_0(\boldsymbol{\omega})| \neq 0$, *then* $(\boldsymbol{\eta}_1 - \boldsymbol{\eta}_6)^\top (\boldsymbol{\pi}_6 - \boldsymbol{\pi}_7) \neq 0 (mod\, 2\pi)$.

Because $m_0(\boldsymbol{\omega})$ can be expressed as in (22), $|m_0(\boldsymbol{\omega})| \neq 0$ is equivalent to $\det(\,\widetilde{\mathbf{M}}^{\square}[-k_{\boldsymbol{\omega}}, :](\boldsymbol{\omega})\,) \neq 0$, i.e. $\widetilde{\mathbf{M}}^{\square}(\boldsymbol{\omega})$ is full rank. The constraint on $\boldsymbol{\eta}_1$ and $\boldsymbol{\eta}_6$ then follows from substituting non-zero entries of $\widetilde{\mathbf{M}}^{\square}(\boldsymbol{\omega})$ by (25) and consider the linear dependency of the columns in $\widetilde{\mathbf{M}}^{\square}(\boldsymbol{\omega})$. For the full proof of Lemma 5.1, see Appendix B.2.

Similarly, if $\exists\, \boldsymbol{\omega} \in \{\omega_1 = \omega_2, \omega_1 \in (0, \frac{\pi}{2})\}$, *s.t.* $|m_0(\boldsymbol{\omega})| \neq 0$, then $(\boldsymbol{\eta}_1 - \boldsymbol{\eta}_6)^\top (\boldsymbol{\pi}_6 - \boldsymbol{\pi}_1) \neq 0 (\mathrm{mod}\, 2\pi)$. These two conditions are equivalent to

$$(\boldsymbol{\eta}_1 - \boldsymbol{\eta}_6)^\top (\pi/2, \pi/2) \neq 0 (\mathrm{mod}\, 2\pi) \tag{c1.1}$$

since $\boldsymbol{\eta}_1$, $\boldsymbol{\eta}_6 \in \mathbb{Z}^2$. Considering the other diagonal segment $\{\omega_2 = -\omega_1, |\omega_1| < \frac{\pi}{2}\}$, we also have

$$(\boldsymbol{\eta}_3 - \boldsymbol{\eta}_4)^\top (-\pi/2, \pi/2) \neq 0 (\mathrm{mod}\, 2\pi) \tag{c1.2}$$

Next, we consider $\widetilde{m_0}(\mathbf{0})$ and investigate $\widetilde{\mathbf{M}}^{\square}(\boldsymbol{\omega})$ at the origin.

Proposition 5.2. *If* $|\widetilde{m_0}(\mathbf{0})| \neq 0$, *then* $\boldsymbol{\pi}_1^\top (\boldsymbol{\eta}_1 - \boldsymbol{\eta}_6) \neq \pi (mod\, 2\pi)$ *or* $\boldsymbol{\pi}_3^\top (\boldsymbol{\eta}_3 - \boldsymbol{\eta}_4) \neq \pi (mod\, 2\pi)$.

Remark. The proof of Proposition 5.2 is similar to that of Lemma 5.1 but more involved. See Appendix B.2 for the full proof.

We propose the following set of phases such that (**c1.1**) and (**c1.2**) as well as the necessary condition from Proposition 5.2 are all satisfied,

$$\begin{aligned} &\boldsymbol{\eta}_1 = (0, 0),\ \boldsymbol{\eta}_2 = (-1, 1),\ \boldsymbol{\eta}_3 = (0, 2), \\ &\boldsymbol{\eta}_4 = (1, 0),\ \boldsymbol{\eta}_5 = (0, -1),\ \boldsymbol{\eta}_6 = (0, 1). \end{aligned} \tag{26}$$

5.2 Solving (18) and (17) for $m_0, \widetilde{m_0}$ and m_j

Once $\widetilde{m_j}(\boldsymbol{\omega}), j = 1, \cdots, 6$ are fixed on S_0, (18) can be reformulated as follows,

$$\widetilde{\mathbf{M}}[:, -0](\boldsymbol{\omega}) \begin{bmatrix} m_1(\boldsymbol{\omega}) \\ m_2(\boldsymbol{\omega}) \\ m_3(\boldsymbol{\omega}) \\ m_4(\boldsymbol{\omega}) \\ m_5(\boldsymbol{\omega}) \\ m_6(\boldsymbol{\omega}) \end{bmatrix} = \boldsymbol{b}_0 - m_0(\boldsymbol{\omega}) \begin{bmatrix} \overline{\widetilde{m_0}}(\boldsymbol{\omega}) \\ 0 \\ \overline{\widetilde{m_0}}(\boldsymbol{\omega} + \boldsymbol{\pi}_2) \\ 0 \\ \overline{\widetilde{m_0}}(\boldsymbol{\omega} + \boldsymbol{\pi}_4) \\ 0 \\ \overline{\widetilde{m_0}}(\boldsymbol{\omega} + \boldsymbol{\pi}_6) \\ 0 \end{bmatrix} \doteq \boldsymbol{b}_0'(\boldsymbol{\omega}), \tag{27}$$

where $\widetilde{\mathbf{M}}[:,-0](\boldsymbol{\omega})$ is completely determined by $\widetilde{m_j}(\boldsymbol{\omega})$, $j=1,\cdots,6$ and m_j, $j=1,\cdots,6$ can be uniquely solved on S_0 if and only if $\forall \boldsymbol{\omega}\in S_0$

(5.2.i) $\widetilde{\mathbf{M}}[:,-0](\boldsymbol{\omega})$ is full rank,

(5.2.ii) $\boldsymbol{b}_0'(\boldsymbol{\omega})$ is in $col\big(\widetilde{\mathbf{M}}[:,-0](\boldsymbol{\omega})\big)$, the column space of $\widetilde{\mathbf{M}}[:,-0](\boldsymbol{\omega})$.

Next, we show that (5.2.ii) breaks down to constraints on two submatrices of $\widetilde{\mathbf{M}}[:,-0](\boldsymbol{\omega})$ and quadruples $\big(m_0(\boldsymbol{\omega}),m_0(\boldsymbol{\omega}+\boldsymbol{\pi}_2),m_0(\boldsymbol{\omega}+\boldsymbol{\pi}_4),m_0(\boldsymbol{\omega}+\boldsymbol{\pi}_6)\big)$, $\big(m_0(\boldsymbol{\omega}+\boldsymbol{\pi}_1),m_0(\boldsymbol{\omega}+\boldsymbol{\pi}_3),m_0(\boldsymbol{\omega}+\boldsymbol{\pi}_5),m_0(\boldsymbol{\omega}+\boldsymbol{\pi}_7)\big)$.

Proposition 5.3. *Let $\widetilde{\mathbf{M}}[odd,-0](\boldsymbol{\omega}),\widetilde{\mathbf{M}}[even,-0](\boldsymbol{\omega})\in\mathbb{C}^{4\times 6}$ be the sub-matrices of $\widetilde{\mathbf{M}}[:,-0](\boldsymbol{\omega})$ consisting of odd and even indexed rows respectively. $\forall\boldsymbol{\omega}\in S_0$, suppose* (5.2.i) *holds, then* (5.2.ii) *holds if and only if* $rank(\,\widetilde{\mathbf{M}}[odd,-0](\boldsymbol{\omega})\,)=rank(\,\widetilde{\mathbf{M}}[even,-0](\boldsymbol{\omega})\,)=3$ *and*

$$[m_0(\boldsymbol{\omega}),m_0(\boldsymbol{\omega}+\boldsymbol{\pi}_2),m_0(\boldsymbol{\omega}+\boldsymbol{\pi}_4),m_0(\boldsymbol{\omega}+\boldsymbol{\pi}_6)]\,\widetilde{\mathbf{M}}[even,-0](\boldsymbol{\omega})=\mathbf{0}, \tag{28}$$

$$[m_0(\boldsymbol{\omega}+\boldsymbol{\pi}_1),m_0(\boldsymbol{\omega}+\boldsymbol{\pi}_3),m_0(\boldsymbol{\omega}+\boldsymbol{\pi}_5),m_0(\boldsymbol{\omega}+\boldsymbol{\pi}_7)]\,\widetilde{\mathbf{M}}[odd,-0](\boldsymbol{\omega})=\mathbf{0}. \tag{29}$$

For the proof of Proposition 5.3, see Appendix B.3.

Remark. Note that the submatrices $\widetilde{\mathbf{M}}[odd,-0](\boldsymbol{\omega})$ and $\widetilde{\mathbf{M}}[even,-0](\boldsymbol{\omega})$ are dual to each other under the shift of variable $\boldsymbol{\omega}\mapsto\boldsymbol{\omega}+\boldsymbol{\pi}_i$, when i is odd. Therefore, the constraints $rank(\,\widetilde{\mathbf{M}}[even,-0](\boldsymbol{\omega})\,)=3$ and (28) from Proposition 5.3 are sufficient for (5.2.ii) to hold on S_0. Furthermore, because $\widetilde{\mathbf{M}}[even,-0](\boldsymbol{\omega})$ and $(\boldsymbol{\omega},\boldsymbol{\omega}+\boldsymbol{\pi}_2,\boldsymbol{\omega}+\boldsymbol{\pi}_4,\boldsymbol{\omega}+\boldsymbol{\pi}_6)$ are invariant to the shift of variable $\boldsymbol{\omega}\mapsto\boldsymbol{\omega}+\boldsymbol{\pi}_i$ when i is even, we only need to consider the constraints above on the subset $[-\pi,0)\times[-\pi,0)$ of S_0.

In sum, $\widetilde{\mathbf{M}}[:,-0](\boldsymbol{\omega})$ (or equivalently $\widetilde{m_j}$) has to satisfy the following rank constraints on $[-\pi,0)\times[-\pi,0)$ for (27) to be uniquely solvable on S_0,

$$rank(\,\widetilde{\mathbf{M}}[:,-0](\boldsymbol{\omega})\,)=6,\ rank(\,\widetilde{\mathbf{M}}[even,-0](\boldsymbol{\omega})\,)=3. \tag{30}$$

As the rank constraints are hard to impose while designing $\widetilde{m_j}$, in our numerical experiments, we check if these rank constraints are satisfied afterwards, see step 1. in Algorithm 1.

Suppose (30) hold, the quadruple $\big(m_0(\boldsymbol{\omega}),m_0(\boldsymbol{\omega}+\boldsymbol{\pi}_2),m_0(\boldsymbol{\omega}+\boldsymbol{\pi}_4),m_0(\boldsymbol{\omega}+\boldsymbol{\pi}_6)\big)$ can then be uniquely determined by (28) *up to a constant* $a_{\boldsymbol{\omega}}$, where its corresponding vector is orthogonal to the column space of $\widetilde{\mathbf{M}}[even,-0](\boldsymbol{\omega})$ of co-dimension 1. In particular, we obtain $m_0(\boldsymbol{\omega})$ on S_0 by solving (28) independently at each $\boldsymbol{\omega}$ on $[-\pi,0)\times[-\pi,0)$, see step 2. in Algorithm 1. Since the constant $a_{\boldsymbol{\omega}}$ can change drastically as $\boldsymbol{\omega}$ changes, there is potential lack of regularity of $m_0(\boldsymbol{\omega})$ as an artifact of the algorithm. Figure 7 shows an $m_0(\boldsymbol{\omega})$ computed in this way, which has discontinuous phase due to $a_{\boldsymbol{\omega}}$. Fortunately, this artificial irregularity can be removed as suggested by the following proposition.

Proposition 5.4. *If $\widetilde{m_j}(\boldsymbol{\omega}),m_j(\boldsymbol{\omega})$, $j=0,1,...,6$ satisfy* (18) *and* (17)*, then $m_0'(\boldsymbol{\omega})\doteq m_0(\boldsymbol{\omega})c(\boldsymbol{\omega}),\widetilde{m_0}'(\boldsymbol{\omega})\doteq\widetilde{m_0}(\boldsymbol{\omega})\bar{c}(\boldsymbol{\omega})^{-1}$ together with the same $m_j(\boldsymbol{\omega}),\widetilde{m_j}(\boldsymbol{\omega})$, $j=1,\cdots,6$ satisfy* (18) *and* (17) *if $c(\boldsymbol{\omega})=c(\boldsymbol{\omega}+\boldsymbol{\pi}_2)=c(\boldsymbol{\omega}+\boldsymbol{\pi}_4)=c(\boldsymbol{\omega}+\boldsymbol{\pi}_6)\neq 0$, i.e. $c(\boldsymbol{\omega})$ is π-periodic in both ω_1 and ω_2.*

Proof. It suffices to show that $m_0'(\boldsymbol{\omega})\overline{\widetilde{m_0}'}(\boldsymbol{\omega}+\boldsymbol{\pi}_i)=m_0(\boldsymbol{\omega})\overline{\widetilde{m_0}}(\boldsymbol{\omega}+\boldsymbol{\pi}_i)$, when i is even. □

Remark. Proposition 5.4 suggests that we can compensate $a_{\boldsymbol{\omega}}$ by choosing $c(\boldsymbol{\omega})$ such that $(m_0',\widetilde{m_0}')$ have improved regularity, e.g. continuity, smoothness or fast decay rate. In practice, we first solve $\widetilde{m_0}(\boldsymbol{\omega})$, step 3. in Algorithm 1, then choose $c(\boldsymbol{\omega})$ π-periodic in both axis and replace $m_0(\boldsymbol{\omega})$ and $\widetilde{m_0}(\boldsymbol{\omega})$ by $m_0'(\boldsymbol{\omega})$ and $\overline{\widetilde{m_0}'}(\boldsymbol{\omega})$ as defined in Proposition 5.4.

To obtain $\widetilde{m_0}(\boldsymbol{\omega})$ on S_0, we solve the identity condition (17) on $[-\pi,0)\times[-\pi,0)$ for the quadruple $(\widetilde{m_0}(\boldsymbol{\omega}),\widetilde{m_0}(\boldsymbol{\omega}+\boldsymbol{\pi}_2),\widetilde{m_0}(\boldsymbol{\omega}+\boldsymbol{\pi}_4),\widetilde{m_0}(\boldsymbol{\omega}+\boldsymbol{\pi}_6))$. Note that (17) is the same as (21) in Section 4.1. According to Lemma 3.2.1 in [10], based on *Hilbert's Nullstellensatz*, (21) has a solution if and only if there does not exist $(z_1,z_2)\in(\mathbb{C}^*)^2$, $\mathbb{C}^*=\mathbb{C}\setminus\{0\}$ s.t. $(\pm z_1,\pm z_2)$ are all vanishing points of the z-transform of m_0. In general, there is no efficient algorithm to solve *Hilbert's Nullstellensatz*, and how (21) is solved exactly is not mentioned in [10].

Here, we reformulate it as an optimization problem wher (17) serves as a linear constraint. In particular, on a $2N\times 2N$ regular grid $\mathcal{G}=\{\boldsymbol{\omega}_i\}_{i=1}^{4N^2}$ of $[-\pi,\pi)\times[-\pi,\pi)$, (17) can be rewritten as

$$\boldsymbol{A}\,\overline{\widetilde{\mathbf{m}_0}}=\mathbf{1}_{4N^2}, \tag{31}$$

where $\widetilde{\mathbf{m}}_0 = [\widetilde{m_0}(\boldsymbol{\omega}_i)]_{i=1}^{4N^2}$ and $\boldsymbol{A} \in \mathbb{C}^{N^2 \times 4N^2}$ is a sparse matrix with entries

$$\boldsymbol{A}_{i,j} = m_0(\boldsymbol{\omega}_j) \sum_{k=0}^{3} \delta(\boldsymbol{\omega}_j - \boldsymbol{\omega}_i - \boldsymbol{\pi}_{2k}), \quad \boldsymbol{\omega}_j \in [-\pi, 0) \times [-\pi, 0).$$

We optimize the regularity of $\overline{\widetilde{m_0}}(\boldsymbol{\omega}) m_0(\boldsymbol{\omega})$ instead of $\overline{\widetilde{m_0}}(\boldsymbol{\omega})$, as this product remains the same for $(\, m_0'(\boldsymbol{\omega}), \widetilde{m_0}'(\boldsymbol{\omega})\,)$ and its regularity controls the regularity of $(\, m_0'(\boldsymbol{\omega}), \widetilde{m_0}'(\boldsymbol{\omega})\,)$ that can be achieved. We choose the squared ℓ_2 norm of the gradient of $\overline{\widetilde{m_0}}(\boldsymbol{\omega}) m_0(\boldsymbol{\omega})$ as the objective function, although other forms of regularity may be imposed by different objective functions.

In sum, we solve the following quadratic minimization problem with linear constraint,

$$\min_{\mathbf{x}} \|\boldsymbol{D}(\mathbf{m}_0 \circ \mathbf{x})\|^2, \quad s.t.\ \boldsymbol{A}\mathbf{x} = \mathbf{1}, \tag{32}$$

where $\boldsymbol{D}$ is the gradient operator, $\circ$ is Hadamard product and $\boldsymbol{A}$ is the linear operator from (17).

Supplementary numerical results on solving $\widetilde{m_0}(\boldsymbol{\omega})$ by optimization are provided in Appendix C, where we test this optimization method on known bi-orthogonal filters m_0 and $\widetilde{m_0}$ and compare the solution from the optimization with the ground truth.

Finally, we plug $m_0(\boldsymbol{\omega})$ and $\widetilde{m_0}(\boldsymbol{\omega})$ into $\boldsymbol{b}_0'(\boldsymbol{\omega})$ on the right of (27) and solve the linear system, which has a guaranteed unique solution.

Algorithm 1. Construction of $m_0, \widetilde{m_0}$ and $\widetilde{m_j}$ in bi-orthogonal basis

Input: $\widetilde{m_j}(\boldsymbol{\omega})$, $j = 1, ..., 6$

step 1. construct $\widetilde{\mathbf{M}}[:, -0](\boldsymbol{\omega})$ on sub-grid $[-\pi, 0) \times [-\pi, 0)$ and check rank constraints (30),

step 2. solve quadruple $\big(m_0(\boldsymbol{\omega}), m_0(\boldsymbol{\omega} + \boldsymbol{\pi}_2), m_0(\boldsymbol{\omega} + \boldsymbol{\pi}_4), m_0(\boldsymbol{\omega} + \boldsymbol{\pi}_6)\big)$ using (28) on $[-\pi, 0) \times [-\pi, 0)$,

step 3. solve the optimization (32) for $\widetilde{m_0}(\boldsymbol{\omega})$ on grid $[-\pi, \pi) \times [-\pi, \pi)$,

step 4. choose π-periodic $c(\boldsymbol{\omega})$ and replace $m_0(\boldsymbol{\omega})$, $\widetilde{m_0}(\boldsymbol{\omega})$ by $m_0'(\boldsymbol{\omega}) = c(\boldsymbol{\omega}) m_0(\boldsymbol{\omega})$ and $\widetilde{m_0}'(\boldsymbol{\omega}) = \widetilde{m_0}(\boldsymbol{\omega}) \overline{c}(\boldsymbol{\omega})^{-1}$,

step 5. solve the reduced linear system (27) for $m_j(\boldsymbol{\omega})$, $j = 1, \cdots, 6$.

To sum up, we propose Algorithm 1 for bi-orthogonal directional filter construction with dyadic quincunx downsampling scheme.

Remark. The order of step 4. and step 5. in Algorithm 1 can be reversed because (27) only depends on $m_0(\boldsymbol{\omega})\overline{\widetilde{m_0}}(\boldsymbol{\omega} + \boldsymbol{\pi}_i)$ when i is even, which remains the same for $m_0'(\boldsymbol{\omega}), \widetilde{m_0}'(\boldsymbol{\omega})$ regardless of $c(\boldsymbol{\omega})$ by construction.

It is not necessary, but we may also manipulate pairs of $(m_j, \widetilde{m_j})$ according to the following generalization of Proposition 5.4.

Proposition 5.5. *If* $\widetilde{m_j}(\boldsymbol{\omega}), m_j(\boldsymbol{\omega})$, $j = 0, 1, ..., 6$ *satisfy* (18) *and* (17), $m_j^c(\boldsymbol{\omega}) \doteq m_j(\boldsymbol{\omega}) c_j(\boldsymbol{\omega}), \widetilde{m_j}^c(\boldsymbol{\omega}) \doteq \widetilde{m_j}(\boldsymbol{\omega}) \overline{c_j}(\boldsymbol{\omega})^{-1}$ $j = 0, \cdots, 6$ *satisfy* (18) *and* (17) *if* $c_0(\boldsymbol{\omega}) = c_0(\boldsymbol{\omega} + \boldsymbol{\pi}_{2k}), \forall k = 0, \cdots, 3$ *and* $c_j(\boldsymbol{\omega}) = c_j(\boldsymbol{\omega} + \boldsymbol{\pi}_k)$, $\forall\ k = 0, \cdots, 7$, $j = 1, \cdots, 6$.

6 Numerical Experiments

In this section, we demonstrate the numerical construction of biorthogonal directional wavelets on a quincunx lattice using our proposed Algorithm 1 implemented in Matlab.

For the input of Algorithm 1, we use $\widetilde{m_j}$ in the form of (25), with phases in (26) and amplitudes $|\widetilde{m_j}|$ shown in Figure 5 constructed as follows. We start with a symmetric $|\widetilde{m_2}|$, then compute $|\widetilde{m_1}|$ and $|\widetilde{m_3}|$ by shearing $|\widetilde{m_2}|$ counter-clockwise and clockwise respectively. $|\widetilde{m_4}|, |\widetilde{m_5}|$ and $|\widetilde{m_6}|$ are obtained by symmetry along the diagonal. This is the same approach used in the shearlet construction [12]. Furthermore, we set $\widetilde{m_j}(\boldsymbol{\omega}) = 0$, $\forall \boldsymbol{\omega} \in C_0 = [-\frac{\pi}{2}, \frac{\pi}{2}) \times [-\frac{\pi}{2}, \frac{\pi}{2})$. and according to Proposition 4.4, we enforce $|\widetilde{m_1}(\frac{\pi}{2}, \frac{\pi}{2})| \neq 0$ and $|\widetilde{m_6}(\frac{\pi}{2}, \frac{\pi}{2})| \neq 0$. As the first step, we numerically verify that this particular design of $\widetilde{m_j}$ satisfies the rank constraints (30).

We proceed to solve $m_0(\boldsymbol{\omega})$ separately for each $\boldsymbol{\omega}$ with an extra degree of freedom of a constant $a_{\boldsymbol{\omega}}$ and the result is shown in Figure 6. The solution $m_0(\boldsymbol{\omega})$ has both inherent irregularity of the bi-orthogonal

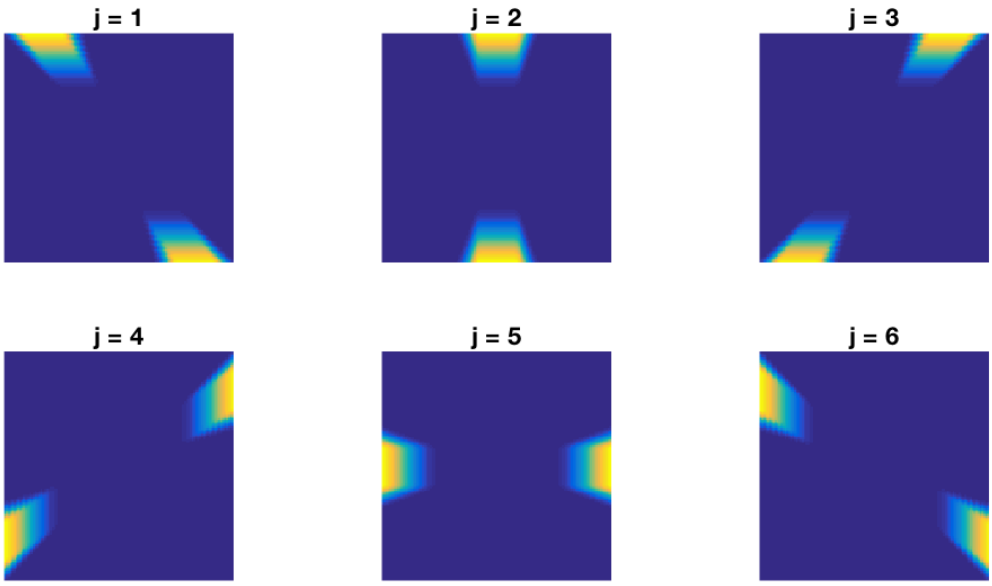

Figure 5: Input $|\widetilde{m_j}(\boldsymbol{\omega})|$ constructed in the same way as shearlets.

construction from the input and artificial irregularity from the algorithm: the amplitude $|m_0(\boldsymbol{\omega})|$ is supported on C_0, where $|m_0(\boldsymbol{\omega})| = 1$ and its discontinuity at ∂C_0 inline with that of the input $\widetilde{m_j}(\boldsymbol{\omega})$; however, the phase of $m_0(\boldsymbol{\omega})$ is discontinuous even on C_0 due to $a_{\boldsymbol{\omega}}$, an artificial irregularity that can be removed after $\widetilde{m_0}(\boldsymbol{\omega})$ is solved, as explained in Section 5.2.

We then solve (32) for $\widetilde{m_0}(\boldsymbol{\omega})$, and the solution is coupled with $m_0(\boldsymbol{\omega})$ in the previous step. The left figure in Figure 7 shows that $\widetilde{m_0}(\boldsymbol{\omega})$ is also supported on C_0 as $m_0(\boldsymbol{\omega})$. This is a result of the linear constraint in (32) from the identity condition (17), not because of the regularization by the objective function where $m_0(\boldsymbol{\omega})\overline{\widetilde{m_0}}(\boldsymbol{\omega}) \equiv 0, \forall \boldsymbol{\omega} \notin C_0$. Furthermore, the middle and right figures in Figure 7 suggest that $m_0(\boldsymbol{\omega})\overline{\widetilde{m_0}}(\boldsymbol{\omega}) = \mathbf{1}_{C_0}$ numerically.

Next, we find $c(\boldsymbol{\omega})$ to obtain $m_0'(\boldsymbol{\omega})$ and $\widetilde{m_0}'(\boldsymbol{\omega})$ with better regularity. We can construct $c(\boldsymbol{\omega})$ freely on C_0 and then extend it to S_0 by its π-periodicity. Since both $m_0(\boldsymbol{\omega})$ and $\widetilde{m_0}(\boldsymbol{\omega})$ are supported on C_0, $m_0'(\boldsymbol{\omega})$ and $\widetilde{m_0}'(\boldsymbol{\omega})$ have the same support as well, thus they are determined by $c(\omega)$ on C_0. Therefore, $m_0'(\boldsymbol{\omega})$ and $\widetilde{m_0}'(\boldsymbol{\omega})$ can be directly obtained by re-decomposition of $m_0(\boldsymbol{\omega})\overline{\widetilde{m_0}}(\boldsymbol{\omega}) = 1$ on C_0. In particular, we let $\widetilde{m_0}'$ be a smooth real function and $m_0'(\boldsymbol{\omega}) = \widetilde{m_0}'(\boldsymbol{\omega})^{-1}$ on C_0, see Figure 8.

Finally, we solve (27) for $\widetilde{m_j}(\boldsymbol{\omega})$. As shown in figure 5, the energy of $\widetilde{m_j}$ concentrates at ∂C_0, where m_j decay to near zero. Moreover, Figure 10 shows that $|m_j\widetilde{m_j}(\boldsymbol{\omega})|$ are close to constant on C_j, which is similar to the energy concentration of m_0' at the corners of C_0 that compensates the decay of m_0' in Figure 8. Such irregularity roots in the irregularity of bi-orthogonal bases construction we show in Section 4.3, which prevents input $\widetilde{m_j}$ to be continuous in the first place. We also numerically verify that $m_j(\boldsymbol{\omega})$ and $\widetilde{m_j}(\boldsymbol{\omega})$ have the same phase, i.e. $\overline{m_j\widetilde{m_j}}(\boldsymbol{\omega}) \in \mathbb{R}$.

So far, we construct a set of $(m_j, \widetilde{m_j})_{j=0,\cdots,6}$ that satisfies (18) and (17), thus it can be used to construct biorthogonal wavelets based on (4) and (14). Figure 11 shows the dual wavelets $\widetilde{\psi^j}$ in (13) constructed using (14). Because of the regularity we impose on $\widetilde{m_j}$ and $\widetilde{m_0}'$, the dual wavelets are spatially localized and have good direction selection. The wavelets and scaling functions in (13) can be constructed using (14) similarly, but with much poorer regularity originated in m_j and m_0'.

Although using a different set of $\widetilde{m_j}$ as input paired with a carefully tweaked $\widetilde{m_0}'$ might improve the regularity of the dual wavelets $\widetilde{\psi^j}$, the intrinsic irregularity of the corresponding wavelets ψ^j shall remain.

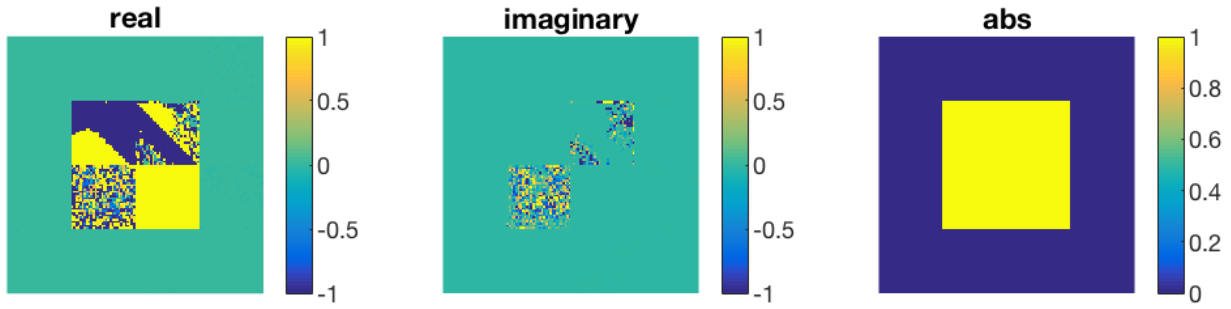

Figure 6: $m_0(\boldsymbol{\omega})$ constructed from $\widetilde{m_j}$. Left to right: $Re(m_0(\boldsymbol{\omega}))$, $Im(m_0(\boldsymbol{\omega}))$ and $|m_0(\boldsymbol{\omega})|$.

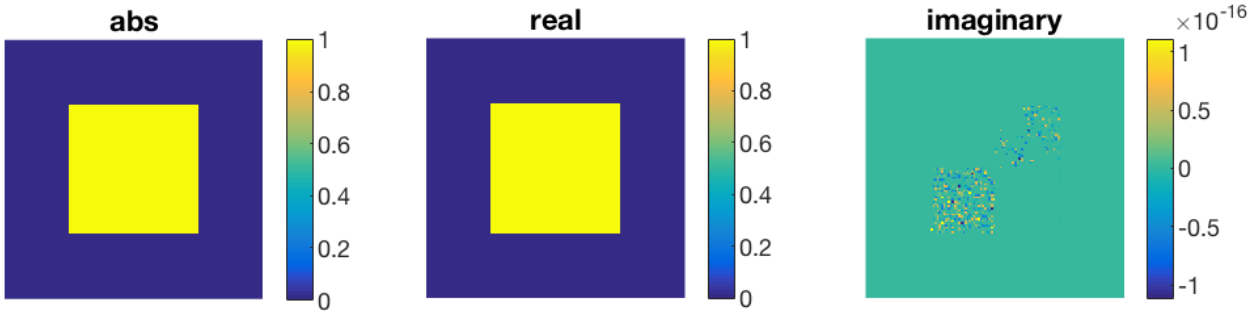

Figure 7: $|\widetilde{m_0}(\boldsymbol{\omega})|$ and $m_0\overline{\widetilde{m_0}}(\boldsymbol{\omega})$, where $\widetilde{m_0}(\boldsymbol{\omega})$ is solved by optimization (32), given $\widetilde{m_j}$ in Figure 5 and m_0 in Figure 6. Left to right: $|\widetilde{m_0}(\boldsymbol{\omega})|$, $Re(m_0\overline{\widetilde{m_0}}(\boldsymbol{\omega}))$ and $Im(m_0\overline{\widetilde{m_0}}(\boldsymbol{\omega}))$.

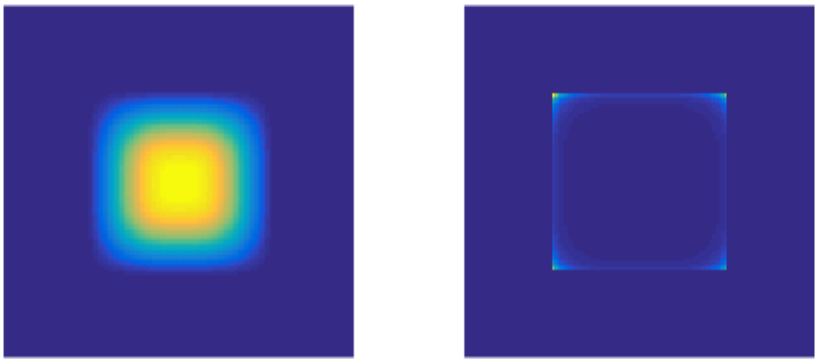

Figure 8: Left: $\widetilde{m_0}'$, designed smooth function mainly supported on the central square C_0, right: m_0', where $m_0'\overline{\widetilde{m_0}'}(\boldsymbol{\omega}) = m_0\overline{\widetilde{m_0}}(\boldsymbol{\omega}) = \mathbf{1}_{C_0}(\boldsymbol{\omega})$.

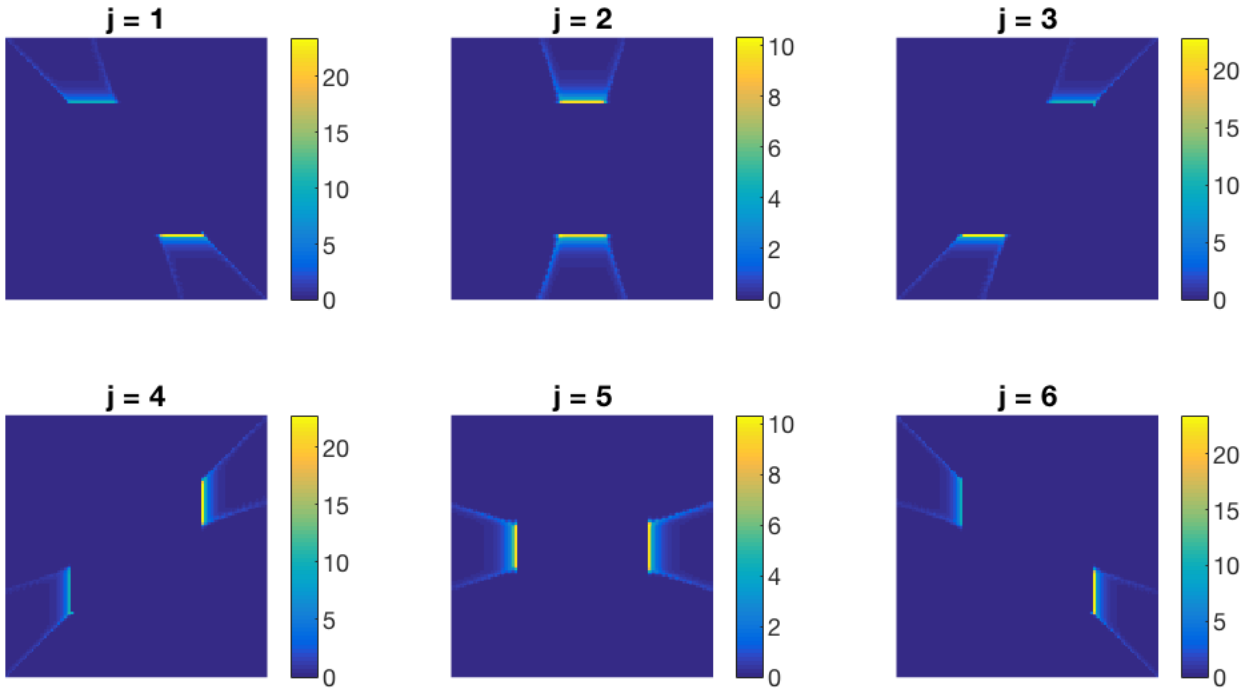

Figure 9: $|m_j(\boldsymbol{\omega})|$, where $m_j(\boldsymbol{\omega})$ is solved from (27) given $\widetilde{m_j}$ in Figure 5, m_0' and $\widetilde{m_0}'$ in Figure 8.

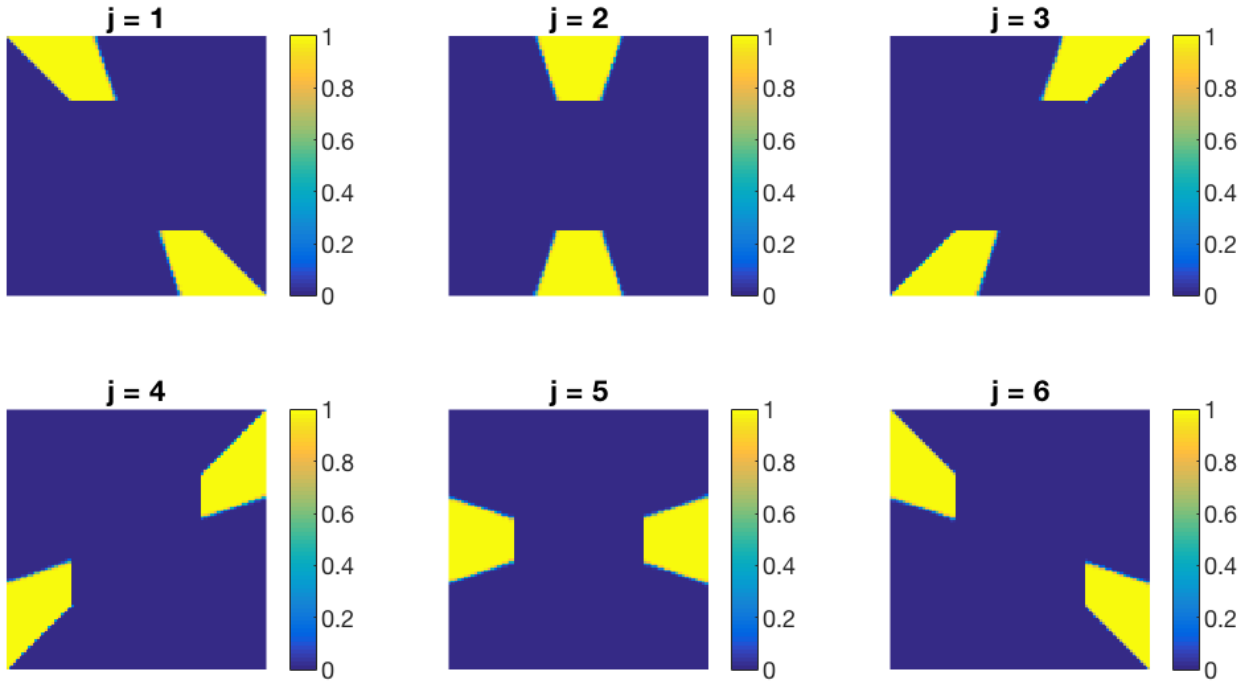

Figure 10: $|m_j(\boldsymbol{\omega})\widetilde{m_j}(\boldsymbol{\omega})|$ for m_j in Figure 9 and $\widetilde{m_j}$ in Figure 5.

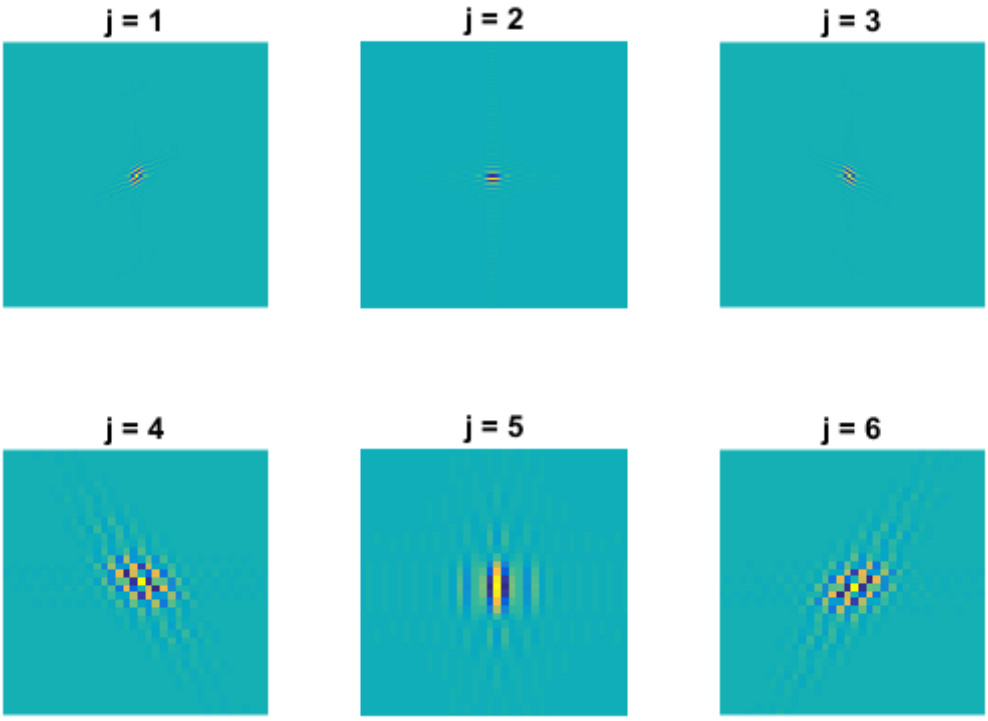

Figure 11: Real part of ψ^j constructed from $\widetilde{m_0}'$ in Figure 8 and $\widetilde{m_j}$, $j = 1, \cdots, 6$ in Figure 5 using (14). Top: $\widetilde{\psi^j}$ without scaling, bottom: $\widetilde{\psi^j}$ with eight time zoom-in

7 Conclusion and future work

In this paper, we consider directional wavelet schemes on dyadic quincunx sub-lattice and analyze their regularity. We show that filters in bi-orthogonal bases have the same discontinuity in the frequency domain as that of the orthonormal bases at the corners of $C_0 = [-\pi/2, \pi/2) \times [-\pi/2, \pi/2)$.

We propose a different approach to construct biorthogonal wavelets from our previous approach for the orthonormal bases construction [9]. The directional dual filters $\widetilde{m_j}$ are first designed such that they can be extended to a bi-orthogonal frame and the remaining filters are obtained by solving linear systems and a constrained quadratic optimization derived from the identity summation and shift cancellation conditions for a biorthogonal MRA. We show numerically, that regularized dual wavelets $\widetilde{\psi^j}$ can be constructed, yet their corresponding wavelets ψ^j are discontinuous in frequency domain, which is unavoidable according to our analysis.

The extension of the biorthogonal bases to low-redundancy dual frame construction is not studied here, which shall achieve at least the same regularity as that of the low-redundancy frame, but with more flexibility in the construction. In addition, our current bi-orthogonal wavelet construction algorithm may be extended to construct low-redundancy dual frames.

Appendices

A Proof of Theorem 1

Take the Fourier transform of both sides of (6), we have

$$\sum_{\boldsymbol{k}}\langle f,\phi_{\boldsymbol{k}}\rangle\hat{\phi}(\boldsymbol{\omega})e^{-i\boldsymbol{\omega}^T\boldsymbol{k}}=\sum_{\boldsymbol{k}}\langle f,\phi_{1,\boldsymbol{k}}\rangle e^{-i\boldsymbol{\omega}^T\boldsymbol{D_2k}}|\boldsymbol{D_2}|^{1/2}\hat{\phi}(\boldsymbol{D_2}^T\boldsymbol{\omega})$$
$$+\sum_{j=1}^{J}\sum_{\boldsymbol{k}}\langle f,\psi^j_{1,\boldsymbol{k}}\rangle e^{-i\boldsymbol{\omega}^T\boldsymbol{Dk}}|\boldsymbol{D}|^{1/2}\hat{\phi}(\boldsymbol{D}^T\boldsymbol{\omega})$$

Suppose m_j are trigonometric series

$$m_0(\boldsymbol{\omega})=\sum_{\boldsymbol{k}}c_{\boldsymbol{k}}e^{-i\boldsymbol{\omega}^T\boldsymbol{k}}\quad m_j(\boldsymbol{\omega})=\sum_{\boldsymbol{k}}g_{\boldsymbol{k}}e^{-i\boldsymbol{\omega}^T\boldsymbol{k}},\quad j=1,\cdots,J \tag{33}$$

The first term on the right hand side can be represented by $\hat{\phi}(\boldsymbol{\omega})$ and $\langle f,\phi_k\rangle$ using (1) and (33).

$$\begin{aligned}\text{the first term on R.H.S. }&=\sum_{\boldsymbol{k}}\langle f,\phi_{1,\boldsymbol{k}}\rangle e^{-i\boldsymbol{\omega}^T\boldsymbol{D_2k}}|\boldsymbol{D_2}|^{1/2}m_0(\boldsymbol{\omega})\hat{\phi}(\boldsymbol{\omega})\\&=\sum_{\boldsymbol{k}}\Big(\sum_{\boldsymbol{k'}}\langle f,\phi_{\boldsymbol{k'}}\rangle\overline{c_{\boldsymbol{k'}-\boldsymbol{D_2k}}}|\boldsymbol{D_2}|^{1/2}\Big)e^{-i\boldsymbol{\omega}^T\boldsymbol{D_2k}}|\boldsymbol{D_2}|^{1/2}m_0(\boldsymbol{\omega})\hat{\phi}(\boldsymbol{\omega})\\&=\sum_{\boldsymbol{k'}}\langle f,\phi_{\boldsymbol{k'}}\rangle\Big(|\boldsymbol{D_2}|\sum_{\boldsymbol{k}}\overline{c_{\boldsymbol{k'}-\boldsymbol{D_2k}}}e^{i\boldsymbol{\omega}^T(\boldsymbol{k'}-\boldsymbol{D_2k})}\Big)e^{-i\boldsymbol{\omega}^T\boldsymbol{k'}}m_0(\boldsymbol{\omega})\hat{\phi}(\boldsymbol{\omega}).\end{aligned}$$

Remark. If we have a shift $\boldsymbol{k}_0$ in the down-sample scheme, i.e. $\boldsymbol{D_2}\mathbb{Z}^2-\boldsymbol{k}_0$ instead of $\boldsymbol{D_2}\mathbb{Z}^2$, so that we obtain coefficient of $\tilde{\phi}_{1,\boldsymbol{k}}=\phi_{1,\boldsymbol{k}+\boldsymbol{k}_0}$ instead of $\phi_{1,\boldsymbol{k}}$, and $\tilde{\phi}_1(\boldsymbol{x})=\phi_1(\boldsymbol{x}-\boldsymbol{k}_0)=|\boldsymbol{D_2}|^{1/2}\sum_{\boldsymbol{k}}c_{\boldsymbol{k}}\phi(\boldsymbol{x}-\boldsymbol{k}-\boldsymbol{k}_0)=|\boldsymbol{D_2}|^{1/2}\sum_{\boldsymbol{k}}c_{\boldsymbol{k}-\boldsymbol{k}_0}\phi(\boldsymbol{x}-\boldsymbol{k})$. This change of down-sample scheme results in an extra phase term $e^{-i\boldsymbol{\omega}^T\boldsymbol{k}_0}$ in m_0. Here, we use the down-sample scheme without translation.

Since $\bigcup_{\boldsymbol{\beta}\in B}\{\boldsymbol{\beta}\}:=\bigcup_{\boldsymbol{\beta}\in B}(\boldsymbol{D_2}\mathbb{Z}^2+\boldsymbol{\beta})=\mathbb{Z}^2$, where $B=\{(0,0),\,(1,0),\,(0,1),\,(1,1)\}$, the summation over $\boldsymbol{k'}\in\mathbb{Z}^2$ can be written as a double sum $\sum_{\boldsymbol{\beta}\in B}\sum_{\boldsymbol{k'}\in\{\boldsymbol{\beta}\}}$,

$$\begin{aligned}&\sum_{\boldsymbol{\beta}\in B}\sum_{\boldsymbol{k'}\in\{\boldsymbol{\beta}\}}\langle f,\phi_{\boldsymbol{k'}}\rangle\sum_{\boldsymbol{k}}\overline{c_{\boldsymbol{k'}-\boldsymbol{D_2k}}}e^{i\boldsymbol{\omega}^T(\boldsymbol{k'}-\boldsymbol{D_2k})}e^{-i\boldsymbol{\omega}^T\boldsymbol{k'}}|\boldsymbol{D_2}|m_0(\boldsymbol{\omega})\hat{\phi}(\boldsymbol{\omega})\\&=\sum_{\boldsymbol{\beta}\in B}\sum_{\boldsymbol{k'}\in\{\boldsymbol{\beta}\}}\langle f,\phi_{\boldsymbol{k'}}\rangle\sum_{\boldsymbol{k}\in\{\boldsymbol{\beta}\}}\overline{c_{\boldsymbol{k}}}e^{i\boldsymbol{\omega}^T\boldsymbol{k}}e^{-i\boldsymbol{\omega}^T\boldsymbol{k'}}|\boldsymbol{D_2}|m_0(\boldsymbol{\omega})\hat{\phi}(\boldsymbol{\omega})\end{aligned}$$

The summation over $\boldsymbol{k}$ in the middle is similar to the trigonometric form of m_0 in (33), but $\boldsymbol{k}$ takes value on the shifted sub-lattice $\{\boldsymbol{\beta}\}$ instead of $\mathbb{Z}^2$. Therefore, the summation equals to instead a linear combination of m_0 with shifts Γ_0,

$$\sum_{\boldsymbol{\pi}\in\Gamma_0}m_0(\boldsymbol{\omega}+\boldsymbol{\pi})\,e^{i\boldsymbol{\beta}^T\boldsymbol{\pi}}=\sum_{\boldsymbol{k}\in\{\boldsymbol{\beta}\}}c_{\boldsymbol{k}}e^{-i\boldsymbol{\omega}^T\boldsymbol{k}} \tag{34}$$

Substitute (34) into the previous expression,

$$\sum_{\boldsymbol{\beta}\in B}\sum_{\boldsymbol{k'}\in\{\boldsymbol{\beta}\}}\langle f,\phi_{\boldsymbol{k'}}\rangle\sum_{\boldsymbol{\pi}\in\Gamma_0}\overline{m_0(\boldsymbol{\omega}+\boldsymbol{\pi})}\,e^{-i\boldsymbol{\beta}^T\boldsymbol{\pi}}\,e^{-i\boldsymbol{\omega}^T\boldsymbol{k'}}m_0(\boldsymbol{\omega})\hat{\phi}(\boldsymbol{\omega})$$

Since $e^{i\boldsymbol{\pi}^T\boldsymbol{\beta}}=e^{i\boldsymbol{\pi}^T\boldsymbol{k'}}$, $\forall\boldsymbol{k'}\in\{\boldsymbol{\beta}\}$, after rewriting the double sum over $\boldsymbol{k'}$ back to a unit sum on $\mathbb{Z}^2$, we get

$$\sum_{\boldsymbol{k'}}\langle f,\phi_{\boldsymbol{k'}}\rangle e^{-i\boldsymbol{\omega}^T\boldsymbol{k'}}\hat{\phi}(\boldsymbol{\omega})\Big(\sum_{\boldsymbol{\pi}\in\Gamma_0}\overline{m_0(\boldsymbol{\omega}+\boldsymbol{\pi})}m_0(\boldsymbol{\omega})e^{-i\boldsymbol{\pi}^T\boldsymbol{k'}}\Big)$$

Similarly, the second term on the R.H.S. of (6) equals to

$$\sum_{j=1}^{J}\sum_{\boldsymbol{k'}}\langle f,\phi_{\boldsymbol{k'}}\rangle e^{-i\boldsymbol{\omega}^T\boldsymbol{k'}}\hat{\phi}(\boldsymbol{\omega})\Big(\sum_{\boldsymbol{\pi}\in\Gamma_1}\overline{m_j(\boldsymbol{\omega}+\boldsymbol{\pi})}m_j(\boldsymbol{\omega})e^{-i\boldsymbol{\pi}^T\boldsymbol{k'}}\Big)$$

(For Theorem 3 on frame construction, the summation of shifts $\boldsymbol{\pi}$ is over Γ_0 instead of Γ_1.) Combining the two terms on the R.H.S. of (6), and compare the coefficients of $\langle f,\phi_{\boldsymbol{k'}}\rangle e^{-i\boldsymbol{\omega}^T\boldsymbol{k'}}\hat{\phi}(\boldsymbol{\omega})$ on both sides, the

perfect reconstruction condition is then equivalent to $\forall \boldsymbol{k}'$,

$$\sum_{\boldsymbol{\pi}\in\Gamma_0} e^{-i\boldsymbol{\pi}^T\boldsymbol{k}'}\overline{m_0(\boldsymbol{\omega}+\boldsymbol{\pi})}m_0(\boldsymbol{\omega}) + \sum_j \sum_{\boldsymbol{\pi}\in\Gamma_1} e^{-i\boldsymbol{\pi}^T\boldsymbol{k}'}\overline{m_j(\boldsymbol{\omega}+\boldsymbol{\pi})}m_j(\boldsymbol{\omega}) = 1.$$

This is equivalent to

$$|m_0(\boldsymbol{\omega})|^2 + \sum_j |m_j(\boldsymbol{\omega})|^2 = 1$$

and

$$\sum_{j=0}^{J} \overline{m_j(\boldsymbol{\omega}+\boldsymbol{\pi})}m_j(\boldsymbol{\omega}) = 0,\ \boldsymbol{\pi}\in\Gamma_0\setminus\{\mathbf{0}\}$$

$$\sum_{j=1}^{J} \overline{m_j(\boldsymbol{\omega}+\boldsymbol{\pi})}m_j(\boldsymbol{\omega}) = 0,\ \boldsymbol{\pi}\in\Gamma_1\setminus\Gamma_0$$

Remark. Because each m_j is $(2\pi, 2\pi)$ periodic, we only need to check the above equality $\forall\boldsymbol{\omega}\in S_0$. If we downsample ψ_1^j on a shifted sub-lattice $\boldsymbol{D}\mathbb{Z}^2-\boldsymbol{k}_j$, we then have an extra phase $e^{i\boldsymbol{\pi}^T\boldsymbol{k}_j}$ before $\overline{m_j(\boldsymbol{\omega}+\boldsymbol{\pi})}m_j(\boldsymbol{\omega})$ in shift cancellation condition. This provides additional freedom in the construction yet it is not substantial.

B Proof of lemmas and propositions for bi-orthogonal schemes

B.1 Discontinuity of $\widetilde{m_j}(\boldsymbol{\omega})$

Lemma B.1. *Define* $d_{i,j}(\boldsymbol{\omega}) = \det([\widetilde{\mathbf{m}}^{k_1}(\boldsymbol{\omega})^\top, \cdots, \widetilde{\mathbf{m}}^{k_6}(\boldsymbol{\omega})^\top])$, *where* $0\le k_1<\cdots<k_6\le 7$, *s.t.* $k_l\neq i,j$. (18) *is solvable* $\forall\boldsymbol{\omega}$ *if and only if*

$$\mathfrak{D}(\omega)\begin{bmatrix}\overline{\widetilde{m_0}}(\boldsymbol{\omega})\\ \overline{\widetilde{m_0}}(\boldsymbol{\omega}+\boldsymbol{\pi}_2)\\ \overline{\widetilde{m_0}}(\boldsymbol{\omega}+\boldsymbol{\pi}_4)\\ \overline{\widetilde{m_0}}(\boldsymbol{\omega}+\boldsymbol{\pi}_6)\end{bmatrix} \doteq \begin{bmatrix}0 & d_{0,2} & d_{0,4} & d_{0,6}\\ -d_{0,2} & 0 & d_{2,4} & d_{2,6}\\ -d_{0,4} & -d_{2,4} & 0 & d_{4,6}\\ -d_{0,6} & -d_{2,6} & -d_{4,6} & 0\end{bmatrix}\begin{bmatrix}\overline{\widetilde{m_0}}(\boldsymbol{\omega})\\ \overline{\widetilde{m_0}}(\boldsymbol{\omega}+\boldsymbol{\pi}_2)\\ \overline{\widetilde{m_0}}(\boldsymbol{\omega}+\boldsymbol{\pi}_4)\\ \overline{\widetilde{m_0}}(\boldsymbol{\omega}+\boldsymbol{\pi}_6)\end{bmatrix} = \begin{bmatrix}0\\0\\0\\0\end{bmatrix}. \tag{35}$$

Proof. By Lemma 4.1 and Lemma 4.2, $\widetilde{\mathbf{M}}[-k,:]$, $k=0,2,4,6$ are singular, The singularity condition on $\widetilde{\mathbf{M}}[-0,:](\boldsymbol{\omega})$ can be rewritten as follows,

$$\begin{aligned}0 &= \det(\widetilde{\mathbf{M}}[-0,:])\\ &= \overline{\widetilde{m_0}}(\boldsymbol{\omega}+\boldsymbol{\pi}_2)\cdot\det(\widetilde{\mathbf{M}}^{\square}[-2,:])\\ &\quad + \overline{\widetilde{m_0}}(\boldsymbol{\omega}+\boldsymbol{\pi}_4)\cdot\det(\widetilde{\mathbf{M}}^{\square}[-4,:]) + \overline{\widetilde{m_0}}(\boldsymbol{\omega}+\boldsymbol{\pi}_6)\cdot\det(\widetilde{\mathbf{M}}^{\square}[-6,:])\\ &= 0\cdot\overline{\widetilde{m_0}}(\boldsymbol{\omega}) \ + \ d_{0,2}\cdot\overline{\widetilde{m_0}}(\boldsymbol{\omega}+\boldsymbol{\pi}_2)\\ &\quad + d_{0,4}\cdot\overline{\widetilde{m_0}}(\boldsymbol{\omega}+\boldsymbol{\pi}_4) \ + \ d_{0,6}\cdot\overline{\widetilde{m_0}}(\boldsymbol{\omega}+\boldsymbol{\pi}_6)\end{aligned} \tag{36}$$

Similarly, the second to fourth equations can be obtained by rewriting the singularity condition on $\widetilde{\mathbf{M}}[-2,:]$, $\widetilde{\mathbf{M}}[-4,:]$ and $\widetilde{\mathbf{M}}[-6,:]$ respectively. □

The identity constraint (17) on m_0 and the singularity condition (35) together imply the following proposition,

Proposition B.2. *Given* $\widetilde{m_i}, i=1,\cdots,6$, (18) *has no solution for* $\widetilde{m_0}$, *if* $\exists\,\omega$, *s.t.* $[m_0(\omega), m_0(\omega+\pi_2), m_0(\omega+\pi_4), m_0(\omega+\pi_6)]$ *is a linear combination of the rows of* $\mathfrak{D}(\omega)$.

Proof of Lemma 4.3:

Lemma 4.3. $\exists\,\rho>0$ *s.t. if* $\widetilde{\mathbf{M}}[-0,:](\boldsymbol{\omega})$ *is singular* $\forall\boldsymbol{\omega}\in S_\rho$, *then* $rank(\widetilde{\mathbf{m}}^1,\widetilde{\mathbf{m}}^7)=1$ *or* $rank(\widetilde{\mathbf{m}}^3,\widetilde{\mathbf{m}}^5)=1$.

Proof. When ρ is small enough, due to the concentration property, $\widetilde{m_i}(\boldsymbol{\omega})$ is zero on all but a few sets $S_\rho+\boldsymbol{\pi}_j$ (see Fig.4 for reference of S_ρ and its shifts), thus $\widetilde{\mathbf{m}}^i(\boldsymbol{\omega})$ is sparse on S_ρ and $\widetilde{\mathbf{M}}[:,-0]$ takes the following

form

$$\widetilde{\mathbf{M}}[:,-0](\boldsymbol{\omega}) = \begin{bmatrix} \widetilde{\mathbf{m}}^0 \\ \widetilde{\mathbf{m}}^1 \\ \widetilde{\mathbf{m}}^2 \\ \widetilde{\mathbf{m}}^3 \\ \widetilde{\mathbf{m}}^4 \\ \widetilde{\mathbf{m}}^5 \\ \widetilde{\mathbf{m}}^6 \\ \widetilde{\mathbf{m}}^7 \end{bmatrix} = \begin{bmatrix} 0 & 0 & 0 & 0 & 0 & 0 \\ * & 0 & 0 & 0 & 0 & * \\ 0 & 0 & 0 & * & * & 0 \\ 0 & 0 & * & * & 0 & 0 \\ 0 & * & * & 0 & 0 & 0 \\ 0 & 0 & * & * & 0 & 0 \\ * & 0 & * & * & 0 & * \\ * & 0 & 0 & 0 & 0 & * \end{bmatrix} \tag{37}$$

where $*$ denote possible non-zero entries. We make the following observation of $\widetilde{\mathbf{m}}^i$:

(i) $\widetilde{\mathbf{m}}^0$ is a zero vector

(ii) $\widetilde{\mathbf{m}}^2$ and $\widetilde{\mathbf{m}}^4$ are linearly independent of each other and the rest of $\widetilde{\mathbf{m}}^i$

(iii) $span\{\widetilde{\mathbf{m}}^1, \widetilde{\mathbf{m}}^7\} \perp span\{\widetilde{\mathbf{m}}^3, \widetilde{\mathbf{m}}^5\}$ and $rank(\widetilde{\mathbf{m}}^1, \widetilde{\mathbf{m}}^7) \leq 2$, $rank(\widetilde{\mathbf{m}}^3, \widetilde{\mathbf{m}}^5) \leq 2$

(iv) $span\{\widetilde{\mathbf{m}}^1, \widetilde{\mathbf{m}}^7, \widetilde{\mathbf{m}}^3, \widetilde{\mathbf{m}}^5, \widetilde{\mathbf{m}}^6\} \leq 4$

Since S_ρ is in the low frequency domain, $m_0(\boldsymbol{\omega}) \neq 0$. (22) then implies that $\det(\widetilde{\mathbf{M}}^{\square}[-k_{\boldsymbol{\omega}}, :]) \neq 0$ hence $\widetilde{\mathbf{M}}^{\square}$ is full rank, or equivantly, $rank(\widetilde{\mathbf{M}}[:,-0]) = 6$. It follows from (ii) and (iv) that $rank(\widetilde{\mathbf{m}}^1, \widetilde{\mathbf{m}}^6, \widetilde{\mathbf{m}}^7, \widetilde{\mathbf{m}}^3, \widetilde{\mathbf{m}}^5) = 4$. On the other hand, (ii) and (iv) imply that

$$rank(\widetilde{\mathbf{M}}^{\square}(\boldsymbol{\omega} + \boldsymbol{\pi}_2)) = rank(\widetilde{\mathbf{m}}^0, \widetilde{\mathbf{m}}^4, \widetilde{\mathbf{m}}^6, \widetilde{\mathbf{m}}^1, \widetilde{\mathbf{m}}^3, \widetilde{\mathbf{m}}^5, \widetilde{\mathbf{m}}^7) = 5$$

and likewise

$$rank(\widetilde{\mathbf{M}}^{\square}(\boldsymbol{\omega} + \boldsymbol{\pi}_4)) = rank(\widetilde{\mathbf{m}}^0, \widetilde{\mathbf{m}}^2, \widetilde{\mathbf{m}}^6, \widetilde{\mathbf{m}}^1, \widetilde{\mathbf{m}}^3, \widetilde{\mathbf{m}}^5, \widetilde{\mathbf{m}}^7) = 5.$$

Therefore, $\det(\widetilde{\mathbf{M}}^{\square}(\boldsymbol{\omega} + \boldsymbol{\pi}_2)) = \det(\widetilde{\mathbf{M}}^{\square}(\boldsymbol{\omega} + \boldsymbol{\pi}_4)) = 0$ and (22) implies $m_0(\boldsymbol{\omega} + \boldsymbol{\pi}_2) = m_0(\boldsymbol{\omega} + \boldsymbol{\pi}_4) = 0$. If $\widetilde{\mathbf{m}}^1$ and $\widetilde{\mathbf{m}}^7$ are linearly independent and so are $\widetilde{\mathbf{m}}^3$ and $\widetilde{\mathbf{m}}^5$, then

$$rank(\widetilde{\mathbf{M}}^{\square}(\boldsymbol{\omega} + \boldsymbol{\pi}_6)) = rank(\widetilde{\mathbf{m}}^2, \widetilde{\mathbf{m}}^4, \widetilde{\mathbf{m}}^1, \widetilde{\mathbf{m}}^3, \widetilde{\mathbf{m}}^5, \widetilde{\mathbf{m}}^7) = 6,$$

hence $m_0(\boldsymbol{\omega} + \boldsymbol{\pi}_6) \neq 0$. Therefore,

$$[m_0(\boldsymbol{\omega}), m_0(\boldsymbol{\omega} + \boldsymbol{\pi}_2), m_0(\boldsymbol{\omega} + \boldsymbol{\pi}_4), m_0(\boldsymbol{\omega} + \boldsymbol{\pi}_6)] = [*, 0, 0, *].$$

In addition, $d_{i,j} = 0$, $\forall (i,j)$ except $(0,6)$, so in (35)

$$\mathfrak{D}(\boldsymbol{\omega}) = [d_{0,6}, 0, 0, 0]^\top [0, 0, 0, 1] + [0, 0, 0, d_{0,6}]^\top [-1, 0, 0, 0].$$

By Proposition B.2, the linear system (18) has no solution $\widetilde{m_0}$ and this proofs the lemma. □

Lemma B.3. *Let* $\widetilde{S_\rho} = S_\rho \cap \{\boldsymbol{\omega} : rank(\,\widetilde{\mathbf{m}}^3(\boldsymbol{\omega}),\, \widetilde{\mathbf{m}}^5(\boldsymbol{\omega})\,) = 1\}$*, if* $\widetilde{m_3}(\boldsymbol{\omega})$ *and* $\widetilde{m_4}(\boldsymbol{\omega})$ *concentrate in* T_3 *and* T_4 *respectively, then* $|\widetilde{S_\rho}| = 0$.

Proof. Let $\widetilde{S_\rho} + \boldsymbol{\pi}_3 = \{\boldsymbol{\omega} + \boldsymbol{\pi}_3, \boldsymbol{\omega} \in \widetilde{S_\rho}\}$ and Ω' be the set symmetric to a set $\Omega \subset S_0$ with respect to the diagonal $\omega_1 = -\omega_2$. If $|\widetilde{S_\rho}| > 0$, by the concentration of $\widetilde{m_3}(\boldsymbol{\omega})$ in T_3, $\forall\, \Omega \subset \widetilde{S_\rho} + \boldsymbol{\pi}_3 \subset T_3$ s.t. $|\Omega| > 0$, $\int_\Omega |\widetilde{m_3}| > \int_{\Omega'} |\widetilde{m_3}|$. Due to the symmetry between $|\widetilde{m_3}|$ and $|\widetilde{m_4}|$ defined in (24), $\int_{\Omega'} |\widetilde{m_3}| = \int_\Omega |\widetilde{m_4}|$. Therefore, $\int_\Omega |\widetilde{m_3}| > \int_\Omega |\widetilde{m_4}|$ which implies that $|\widetilde{m_3}(\boldsymbol{\omega})| > |\widetilde{m_4}(\boldsymbol{\omega})|$ *a.e.* on $\widetilde{S_\rho} + \boldsymbol{\pi}_3$ or equivalently $|\widetilde{m_3}(\boldsymbol{\omega} + \boldsymbol{\pi}_3)| > |\widetilde{m_4}(\boldsymbol{\omega} + \boldsymbol{\pi}_3)|$ *a.e.* on $\widetilde{S_\rho}$. Similarly, we have $|\widetilde{m_4}(\boldsymbol{\omega} + \boldsymbol{\pi}_5)| > |\widetilde{m_3}(\boldsymbol{\omega} + \boldsymbol{\pi}_5)|$ *a.e.* on $\widetilde{S_\rho}$ following the same analysis on $\widetilde{S_\rho} + \boldsymbol{\pi}_5 \subset T_4$. On the other hand, $rank(\,\widetilde{\mathbf{m}}^3(\boldsymbol{\omega}),\, \widetilde{\mathbf{m}}^5(\boldsymbol{\omega})\,) = 1$ on $\widetilde{S_\rho}$, hence $\widetilde{m_3}(\boldsymbol{\omega} + \boldsymbol{\pi}_3)\widetilde{m_4}(\boldsymbol{\omega} + \boldsymbol{\pi}_5) = \widetilde{m_3}(\boldsymbol{\omega} + \boldsymbol{\pi}_5)\widetilde{m_4}(\boldsymbol{\omega} + \boldsymbol{\pi}_3)$, which contradicts the previous two inequalities. □

Lemma B.4. *If* $\widetilde{m_1}(\boldsymbol{\omega})$ $(\widetilde{m_6}(\boldsymbol{\omega}))$ *concentrates in* $T_1(T_6)$*, then* $|\widetilde{m_6}(\boldsymbol{\omega})| > |\widetilde{m_1}(\boldsymbol{\omega})|$ *a.e. on* $T_6 \bigcap supp(\widetilde{m_6})$ $(|\widetilde{m_1}(\boldsymbol{\omega})| > |\widetilde{m_6}(\boldsymbol{\omega})|$ a.e. on $T_1 \bigcap \mathrm{supp}(\widetilde{m_1}))$.

Proof. Let $B_6 = \{\boldsymbol{\omega} : |\widetilde{m_6}(\boldsymbol{\omega})| \leq |\widetilde{m_1}(\boldsymbol{\omega})|\} \bigcap T_6 \bigcap supp(\widetilde{m_1})$ and B_1 be the set symmetric to B_6 with respect to $\omega_1 = \omega_2$ and suppose $|B_6| > 0$, then $\int_{B_6} |\widetilde{m_6}(\boldsymbol{\omega})| \leq \int_{B_6} |\widetilde{m_1}(\boldsymbol{\omega})|$. On the other hand, since $\widetilde{m_1}(\boldsymbol{\omega})$ concentrates in T_1, we know $\int_{B_1} |\widetilde{m_1}(\boldsymbol{\omega})| > \int_{B_6} |\widetilde{m_1}(\boldsymbol{\omega})|$. Moreover, due to the symmetry of $\widetilde{m_1}(\boldsymbol{\omega}), \widetilde{m_6}(\boldsymbol{\omega})$ and B_1, B_6, $\int_{B_1} |\widetilde{m_1}(\boldsymbol{\omega})| = \int_{B_6} |\widetilde{m_6}(\boldsymbol{\omega})|$, hence $\int_{B_6} |\widetilde{m_1}(\boldsymbol{\omega})| \geq \int_{B_6} |\widetilde{m_6}(\boldsymbol{\omega})| = \int_{B_1} |\widetilde{m_1}(\boldsymbol{\omega})|$ which results in contradiction. □

Proposition B.5. *If m_1 (m_6) concentrates within T_1 (T_6), then $\widetilde{m_1}(\boldsymbol{\omega}) = \widetilde{m_6}(\boldsymbol{\omega}) = 0$, a.e. on $S_\rho + \boldsymbol{\pi}_1$.*

Proof. Consider frequency domain $S'_\rho = S_\rho \bigcap \{\omega_1 < \omega_2\}$. By Lemma 4.3, $\exists\, \alpha_{\boldsymbol{\omega}} \in \mathbb{C}, s.t.\, \widetilde{\mathbf{m}}^1(\boldsymbol{\omega}) = \alpha_{\boldsymbol{\omega}}\, \widetilde{\mathbf{m}}^7(\boldsymbol{\omega})$, $\forall\, \boldsymbol{\omega} \in S'_\rho$, i.e. $\widetilde{m_1}(\boldsymbol{\omega} + \boldsymbol{\pi}_1) = \alpha_{\boldsymbol{\omega}} \cdot \widetilde{m_1}(\boldsymbol{\omega} + \boldsymbol{\pi}_7)$ and $\widetilde{m_6}(\boldsymbol{\omega} + \boldsymbol{\pi}_1) = \alpha_{\boldsymbol{\omega}} \cdot \widetilde{m_6}(\boldsymbol{\omega} + \boldsymbol{\pi}_7)$. On the other hand, Lemma B.4 implies that $|\widetilde{m_1}(\boldsymbol{\omega} + \boldsymbol{\pi}_7)| \geq |\widetilde{m_6}(\boldsymbol{\omega} + \boldsymbol{\pi}_7)|$, hence $|\widetilde{m_1}(\boldsymbol{\omega} + \boldsymbol{\pi}_1)| \geq |\widetilde{m_6}(\boldsymbol{\omega} + \boldsymbol{\pi}_1)|$. Let $\Omega'_6 \doteq (S_\rho + \boldsymbol{\pi}_1) \bigcap T_6$, then $\int_{\Omega'_6} |\widetilde{m_1}(\boldsymbol{\omega})| \geq \int_{\Omega'_6} |\widetilde{m_6}(\boldsymbol{\omega})|$, which will contradict Lemma B.4 unless $|\Omega'_6 \bigcap \mathrm{supp}(\widetilde{m_6})| = 0$, or equivalently $\alpha_{\boldsymbol{\omega}} = 0$ and so $\widetilde{m_6}(\boldsymbol{\omega}) = \widetilde{m_1}(\boldsymbol{\omega}) = 0$, *a.e.* on Ω'_6. By symmetry, $\widetilde{m_6}(\boldsymbol{\omega}) = \widetilde{m_1}(\boldsymbol{\omega}) = 0$, *a.e.* on $(S_\rho + \boldsymbol{\pi}_1) \setminus \Omega'_6$ as well. □

B.2 Design of input $\widetilde{m_j}(\boldsymbol{\omega})$

Proof of Lemma 5.1:

Lemma 5.1. *If $\exists\, \boldsymbol{\omega} \in D_1 := \{\omega_1 = \omega_2, \omega_1 \in (-\frac{\pi}{2}, 0)\}$, s.t. $m_0(\boldsymbol{\omega}) > 0$, then $(\boldsymbol{\eta}_1 - \boldsymbol{\eta}_6)^\top (\boldsymbol{\pi}_6 - \boldsymbol{\pi}_7) \neq 0 (mod\, 2\pi)$.*

Proof. As $\widetilde{m_1}(\boldsymbol{\omega})$ and $\widetilde{m_6}(\boldsymbol{\omega})$ concentrate in T_1 and T_6 respectively, $\widetilde{m_1}(\boldsymbol{\omega} + \boldsymbol{\pi}_i) = 0$ and $\widetilde{m_6}(\boldsymbol{\omega} + \boldsymbol{\pi}_i) = 0$, $i = 1, \cdots, 5$. Due to symmetry, $|\widetilde{m_1}(\boldsymbol{\omega})| = |\widetilde{m_6}(\boldsymbol{\omega})|$ on $\{\omega_1 = \omega_2\}$. Let $A = |\widetilde{m_1}(\boldsymbol{\omega} + \boldsymbol{\pi}_7)| = |\widetilde{m_6}(\boldsymbol{\omega} + \boldsymbol{\pi}_7)|$ and $B = |\widetilde{m_1}(\boldsymbol{\omega} + \boldsymbol{\pi}_6)| = |\widetilde{m_6}(\boldsymbol{\omega} + \boldsymbol{\pi}_6)|$, then the first and the last columns of $\widetilde{\mathbf{M}}^\square$ are

$$\widetilde{\mathbf{M}}^\square[:, 1] = \begin{bmatrix} 0 \\ \vdots \\ 0 \\ A e^{i \boldsymbol{\eta}_1^\top (\boldsymbol{\omega} + \boldsymbol{\pi}_6)} \\ B e^{i \boldsymbol{\eta}_1^\top (\boldsymbol{\omega} + \boldsymbol{\pi}_7)} \end{bmatrix} \quad \text{and} \quad \widetilde{\mathbf{M}}^\square[:, 6] = \begin{bmatrix} 0 \\ \vdots \\ 0 \\ A e^{i \boldsymbol{\eta}_6^\top (\boldsymbol{\omega} + \boldsymbol{\pi}_6)} \\ B e^{i \boldsymbol{\eta}_6^\top (\boldsymbol{\omega} + \boldsymbol{\pi}_7)} \end{bmatrix}.$$

By (22), if $m_0(\boldsymbol{\omega}) > 0$, $\boldsymbol{\omega} \in D_1$ then $\widetilde{\mathbf{M}}^\square(\boldsymbol{\omega})$ is full rank, hence its columns are linearly independent. In particular, $\widetilde{\mathbf{M}}^\square[:, 1]$ and $\widetilde{\mathbf{M}}^\square[:, 6]$ are linearly independent, which implies that $e^{i(\boldsymbol{\eta}_1^\top \boldsymbol{\pi}_6 + \boldsymbol{\eta}_6^\top \boldsymbol{\pi}_7)} \neq e^{i(\boldsymbol{\eta}_6^\top \boldsymbol{\pi}_6 + \boldsymbol{\eta}_1^\top \boldsymbol{\pi}_7)}$or equivalently $(\boldsymbol{\eta}_1 - \boldsymbol{\eta}_6)^\top (\boldsymbol{\pi}_6 - \boldsymbol{\pi}_7) \neq 0 (\mathrm{mod} 2\pi)$. □

Proof of Proposition 5.2

Proposition 5.2. *If $\widetilde{m_0}(\mathbf{0}) \neq 0$, then $\boldsymbol{\pi}_1^\top (\boldsymbol{\eta}_1 - \boldsymbol{\eta}_6) \neq \pi (mod\, 2\pi)$ or $\boldsymbol{\pi}_3^\top (\boldsymbol{\eta}_3 - \boldsymbol{\eta}_4) \neq \pi (mod\, 2\pi)$. Proof.* Since $\widetilde{m_0}(\mathbf{0}) \neq 0$, as shown in Lemma 4.3, at $\boldsymbol{\omega} = \mathbf{0}$ $rank(\widetilde{\mathbf{m}}^1, \widetilde{\mathbf{m}}^6, \widetilde{\mathbf{m}}^7, \widetilde{\mathbf{m}}^3, \widetilde{\mathbf{m}}^5) = 4$. This is equivalent to the matrix $\boldsymbol{A}$ defined in (38) to be full rank.

$$\boldsymbol{A} = \begin{bmatrix} \widetilde{m_1}(\boldsymbol{\pi}_6) & \widetilde{m_6}(\boldsymbol{\pi}_6) & \widetilde{m_3}(\boldsymbol{\pi}_6) & \widetilde{m_4}(\boldsymbol{\pi}_6) \\ \widetilde{m_1}(\boldsymbol{\pi}_1) & \widetilde{m_6}(\boldsymbol{\pi}_1) & 0 & 0 \\ \widetilde{m_1}(\boldsymbol{\pi}_7) & \widetilde{m_6}(\boldsymbol{\pi}_7) & 0 & 0 \\ 0 & 0 & \widetilde{m_3}(\boldsymbol{\pi}_3) & \widetilde{m_4}(\boldsymbol{\pi}_3) \\ 0 & 0 & \widetilde{m_3}(\boldsymbol{\pi}_5) & \widetilde{m_4}(\boldsymbol{\pi}_5) \end{bmatrix} \tag{38}$$

Let $|\widetilde{m_1}(\boldsymbol{\pi}_1)| = a$, $|\widetilde{m_1}(\boldsymbol{\pi}_6)| = b$. Due to the symmetry of $\widetilde{m_j}(\boldsymbol{\omega})$, $|\widetilde{m_1}(\boldsymbol{\pi}_1)| = |\widetilde{m_1}(\boldsymbol{\pi}_7)| = |\widetilde{m_6}(\boldsymbol{\pi}_1)| = |\widetilde{m_6}(\boldsymbol{\pi}_7)| = |\widetilde{m_3}(\boldsymbol{\pi}_3)| = |\widetilde{m_3}(\boldsymbol{\pi}_5)| = |\widetilde{m_4}(\boldsymbol{\pi}_3)| = |\widetilde{m_4}(\boldsymbol{\pi}_5)|$ and $|\widetilde{m_1}(\boldsymbol{\pi}_6)| = |\widetilde{m_6}(\boldsymbol{\pi}_6)| = |\widetilde{m_3}(\boldsymbol{\pi}_6)| = |\widetilde{m_4}(\boldsymbol{\pi}_6)|$. Rewrite $\boldsymbol{A}$ as follows,

$$\boldsymbol{A} = \begin{bmatrix} b e^{-i \boldsymbol{\pi}_6^\top \boldsymbol{\eta}_1} & b e^{-i \boldsymbol{\pi}_6^\top \boldsymbol{\eta}_6} & b e^{-i \boldsymbol{\pi}_6^\top \boldsymbol{\eta}_3} & b e^{-i \boldsymbol{\pi}_6^\top \boldsymbol{\eta}_4} \\ a e^{-i \boldsymbol{\pi}_1^\top \boldsymbol{\eta}_1} & a e^{-i \boldsymbol{\pi}_1^\top \boldsymbol{\eta}_6} & 0 & 0 \\ a e^{i \boldsymbol{\pi}_1^\top \boldsymbol{\eta}_1} & a e^{i \boldsymbol{\pi}_1^\top \boldsymbol{\eta}_6} & 0 & 0 \\ 0 & 0 & a e^{-i \boldsymbol{\pi}_3^\top \boldsymbol{\eta}_3} & a e^{-i \boldsymbol{\pi}_3^\top \boldsymbol{\eta}_4} \\ 0 & 0 & a e^{i \boldsymbol{\pi}_3^\top \boldsymbol{\eta}_3} & a e^{i \boldsymbol{\pi}_3^\top \boldsymbol{\eta}_4} \end{bmatrix}$$

The product of singular values of $\boldsymbol{A}$ is

$$\sqrt{\det(\boldsymbol{A}^* \boldsymbol{A})} = 4a^3 \sqrt{a^2 K_1^2 K_2^2 + b^2 (Q_1 K_2^2 + Q_2 K_1^2)}, \tag{39}$$

where $Q_1 = 1 - \cos(\boldsymbol{\pi}_6^\top (\boldsymbol{\eta}_1 - \boldsymbol{\eta}_6)) \cos(\boldsymbol{\pi}_1^\top (\boldsymbol{\eta}_1 - \boldsymbol{\eta}_6))$, $Q_2 = 1 - \cos(\boldsymbol{\pi}_6^\top (\boldsymbol{\eta}_3 - \boldsymbol{\eta}_4)) \cos(\boldsymbol{\pi}_3^\top (\boldsymbol{\eta}_3 - \boldsymbol{\eta}_4))$, $K_1 = \sin(\boldsymbol{\pi}_1^\top (\boldsymbol{\eta}_1 - \boldsymbol{\eta}_6))$, $K_2 = \sin(\boldsymbol{\pi}_3^\top (\boldsymbol{\eta}_3 - \boldsymbol{\eta}_4))$. If $\boldsymbol{\pi}_1^\top (\boldsymbol{\eta}_1 - \boldsymbol{\eta}_6) = \boldsymbol{\pi}_3^\top (\boldsymbol{\eta}_3 - \boldsymbol{\eta}_4) = \pi (mod\, 2\pi)$, then $K_1 = K_2 = 0$ and $\boldsymbol{A}$ becomes singular. □

B.3 Solving (18) and (17) for $m_0, \widetilde{m_0}$ and m_j

Lemma B.6. *Let $\boldsymbol{P} \in \mathbb{C}^{n\times n}$ be a projection matrix of rank 2 and $\boldsymbol{a}, \boldsymbol{b}, \boldsymbol{a}', \boldsymbol{b}' \in \mathbb{C}^n$, s.t. $\boldsymbol{a}^*\boldsymbol{b} = (\boldsymbol{a}')^*\boldsymbol{b}' = 1$, $\boldsymbol{a}'^*\boldsymbol{b} = \boldsymbol{a}^*\boldsymbol{b}' = \boldsymbol{b}^*\boldsymbol{b}' = 0$. If $\boldsymbol{P}(\boldsymbol{I}_n - \boldsymbol{a}\otimes\boldsymbol{b} - \boldsymbol{a}'\otimes\boldsymbol{b}') = \boldsymbol{0}$, then $\boldsymbol{P}$ is the projection of span$\{\boldsymbol{b}, \boldsymbol{b}'\}$.*

Proof. Since

$$rank(\boldsymbol{I}_n) \le rank(\boldsymbol{I}_n - \boldsymbol{a}\otimes\boldsymbol{b} - \boldsymbol{a}'\otimes\boldsymbol{b}') + rank(\boldsymbol{a}\otimes\boldsymbol{b}) + rank(\boldsymbol{a}'\otimes\boldsymbol{b}'),$$

it follows that $rank(\boldsymbol{I}_n - \boldsymbol{a}\otimes\boldsymbol{b} - \boldsymbol{a}'\otimes\boldsymbol{b}') \ge n-2$. On the other hand, because $rank(\boldsymbol{P}) = 2$, $\boldsymbol{P}(\boldsymbol{I}_n - \boldsymbol{a}\otimes\boldsymbol{b} - \boldsymbol{a}'\otimes\boldsymbol{b}') = \boldsymbol{0}$ implies that $rank(\boldsymbol{I}_n - \boldsymbol{a}\otimes\boldsymbol{b} - \boldsymbol{a}'\otimes\boldsymbol{b}') \le n-2$. Hence $rank(\boldsymbol{I}_n - \boldsymbol{a}\otimes\boldsymbol{b} - \boldsymbol{a}'\otimes\boldsymbol{b}') = n-2$ and $\boldsymbol{P}$ is the projection of $col(\boldsymbol{I}_n - \boldsymbol{a}\otimes\boldsymbol{b} - \boldsymbol{a}'\otimes\boldsymbol{b}')^\perp$. On the other hand,

$$\begin{aligned}\boldsymbol{b}^*(\boldsymbol{I}_n - \boldsymbol{a}\otimes\boldsymbol{b} - \boldsymbol{a}'\otimes\boldsymbol{b}') &= \boldsymbol{b}^* - (\boldsymbol{b}^*\boldsymbol{a})\boldsymbol{b}^* - (\boldsymbol{b}^*\boldsymbol{a}')(\boldsymbol{b}')^*\\ &= \boldsymbol{b}^* - \boldsymbol{b}^* - 0\cdot(\boldsymbol{b}')^* = \boldsymbol{0}^*\end{aligned}$$

Therefore, $\boldsymbol{P}\boldsymbol{b} = \boldsymbol{b}$. Similarly, $(\boldsymbol{b}')^*(\boldsymbol{I}_n - \boldsymbol{a}\otimes\boldsymbol{b} - \boldsymbol{a}'\otimes\boldsymbol{b}') = \boldsymbol{0}^*$ and $\boldsymbol{P}\boldsymbol{b}' = \boldsymbol{b}'$. Moreover, as $\boldsymbol{b}^*\boldsymbol{b}' = 0$ and $rank(\boldsymbol{P}) = 2$, $\boldsymbol{P} = \|\boldsymbol{b}\|^{-2}\cdot\boldsymbol{b}\otimes\boldsymbol{b} + \|\boldsymbol{b}'\|^{-2}\cdot\boldsymbol{b}'\otimes\boldsymbol{b}'$. □

Lemma B.7. *Given $\widetilde{\mathbf{M}}[:,-0](\boldsymbol{\omega})$ is full rank $\forall\boldsymbol{\omega}$, $\widetilde{\mathbf{M}}[-0,:](\boldsymbol{\omega})$ is singular if (17) holds.*

Proof. If (17) holds, then by Lemma B.6, $\mathbf{m}_0^{\mathcal{E}}$, $\mathbf{m}_0^{\mathcal{O}}$ are orthogonal to $col(\widetilde{\mathbf{M}}[:,-0])$, therefore $\big[\,\mathbf{m}_0^{\mathcal{O}}, \mathbf{m}_0^{\mathcal{E}}, \widetilde{\mathbf{M}}[:,-0]\,\big] \in \mathbb{C}^{8\times 8}$ is full rank. Due to (17), $\mathbf{m}_0^{\mathcal{E}}$ and $\overline{\widetilde{\mathbf{m}_0}}^{\mathcal{E}}$ are not orthogonal to each other, hence $\big[\,\mathbf{m}_0^{\mathcal{O}}, \overline{\widetilde{\mathbf{m}_0}}^{\mathcal{E}}, \widetilde{\mathbf{M}}[:,-0]\,\big] = \big[\,\mathbf{m}_0^{\mathcal{O}}, \widetilde{\mathbf{M}}\,\big]$ is full rank as well. Because $(\mathbf{m}_0^{\mathcal{O}})^*\widetilde{\mathbf{M}}[:,i] = 0$, $i = 0,\cdots,7$ and $\mathbf{m}_0^{\mathcal{O}}[-0]^*\widetilde{\mathbf{M}}[-0,i] = (\mathbf{m}_0^{\mathcal{O}})^*\widetilde{\mathbf{M}}[:,i]$, $\mathbf{m}_0^{\mathcal{O}}[-0]$ is orthogonal to $col(\widetilde{\mathbf{M}}[-0,:])$. Since $\big[\mathbf{m}_0^{\mathcal{O}}[-0], \widetilde{\mathbf{M}}[-0,:]\,\big] \in \mathbb{C}^{7\times 8}$ is full rank, $\widetilde{\mathbf{M}}[-0,:]$ must be singular. □

Proof of Proposition 5.3:

Proposition 5.3. *Let $\widetilde{\mathbf{M}}[odd,-0], \widetilde{\mathbf{M}}[even,-0] \in \mathbb{C}^{4\times 6}$ be the sub-matrices of $\widetilde{\mathbf{M}}[:,-0]$ consisting of odd and even rows respectively. Suppose (5.2.i) holds, then (5.2.ii) holds if and only if $rank(\widetilde{\mathbf{M}}[odd,-0]) = rank(\widetilde{\mathbf{M}}[even,-0]) = 3$ and*

$$[m_0(\boldsymbol{\omega}), m_0(\boldsymbol{\omega}+\boldsymbol{\pi}_2), m_0(\boldsymbol{\omega}+\boldsymbol{\pi}_4), m_0(\boldsymbol{\omega}+\boldsymbol{\pi}_6)]\,\widetilde{\mathbf{M}}[even,-0](\boldsymbol{\omega}) = \boldsymbol{0}, \tag{28}$$

$$[m_0(\boldsymbol{\omega}+\boldsymbol{\pi}_1), m_0(\boldsymbol{\omega}+\boldsymbol{\pi}_3), m_0(\boldsymbol{\omega}+\boldsymbol{\pi}_5), m_0(\boldsymbol{\omega}+\boldsymbol{\pi}_7)]\,\widetilde{\mathbf{M}}[odd,-0](\boldsymbol{\omega}) = \boldsymbol{0}. \tag{29}$$

Proof. Note that $\widetilde{\mathbf{M}}[:,-0]$ have the same rows at $\boldsymbol{\omega}+\boldsymbol{\pi}_i$, $i = 0,\cdots,7$, we define row permutation matrix $\boldsymbol{P}_i$, *s.t.* $\boldsymbol{P}_i\big(\widetilde{\mathbf{M}}[:,-0](\boldsymbol{\omega}+\boldsymbol{\pi}_i)\big) = \widetilde{\mathbf{M}}[:,-0](\boldsymbol{\omega})$. Let $\boldsymbol{P}_{\widetilde{\mathbf{M}}}(\boldsymbol{\omega})$ be the projection matrix of the $col\big(\widetilde{\mathbf{M}}[:,-0](\boldsymbol{\omega})\big)^\perp = null(\widetilde{\mathbf{M}}[:,-0]^*)$, then (5.2.ii) is equivalent to $\boldsymbol{P}_{\widetilde{\mathbf{M}}}\boldsymbol{b}_0'(\boldsymbol{\omega}) = \boldsymbol{0}$. Group this equality at $\boldsymbol{\omega}+\boldsymbol{\pi}_i$, we have

$$\begin{aligned}\boldsymbol{0} &= [\boldsymbol{P}_i\boldsymbol{P}_{\widetilde{\mathbf{M}}}\boldsymbol{b}_0'(\boldsymbol{\omega}+\boldsymbol{\pi}_i)]_{i=0,\cdots,7}\\ &= [\boldsymbol{P}_i\boldsymbol{P}_{\widetilde{\mathbf{M}}}(\boldsymbol{\omega}+\boldsymbol{\pi}_i)\boldsymbol{P}_i^2\boldsymbol{b}_0'(\boldsymbol{\omega}+\boldsymbol{\pi}_i)]_{i=0,\cdots,7}\\ &= [\boldsymbol{P}_{\widetilde{\mathbf{M}}}(\boldsymbol{\omega})\boldsymbol{P}_i\boldsymbol{b}_0'(\boldsymbol{\omega}+\boldsymbol{\pi}_i)]_{i=0,\cdots,7}\\ &= \boldsymbol{P}_{\widetilde{\mathbf{M}}}(\boldsymbol{\omega})[\boldsymbol{P}_i\boldsymbol{b}_0'(\boldsymbol{\omega}+\boldsymbol{\pi}_i)]_{i=0,\cdots,7}\end{aligned} \tag{40}$$

Let

$$\begin{aligned}\overline{\widetilde{\mathbf{m}_0}}^{\mathcal{E}} &= [(1+i \bmod 2)\cdot\overline{\widetilde{m_0}}(\boldsymbol{\omega}+\boldsymbol{\pi}_i)]_{i=0,\cdots,7}^\top = \widetilde{\mathbf{M}}[:,0](\boldsymbol{\omega}),\\ \overline{\widetilde{\mathbf{m}_0}}^{\mathcal{O}} &= [(i \bmod 2)\cdot\overline{\widetilde{m_0}}(\boldsymbol{\omega}+\boldsymbol{\pi}_i)]_{i=0,\cdots,7}^\top,\\ \mathbf{m}_0^{\mathcal{E}} &= [(1+i \bmod 2)\cdot m_0(\boldsymbol{\omega}+\boldsymbol{\pi}_i)]_{i=0,\cdots,7}^\top,\\ \mathbf{m}_0^{\mathcal{O}} &= [(i \bmod 2)\cdot m_0(\boldsymbol{\omega}+\boldsymbol{\pi}_i)]_{i=0,\cdots,7}^\top.\end{aligned}$$

The identity constraint (17) thus can be written as $(\overline{\mathbf{m}_0^{\mathcal{E}}})^*\,\overline{\widetilde{\mathbf{m}_0}}^{\mathcal{E}} = 1$ and $(\overline{\mathbf{m}_0^{\mathcal{O}}})^*\,\overline{\widetilde{\mathbf{m}_0}}^{\mathcal{O}} = 1$. By definition,

$$\boldsymbol{P}_i\boldsymbol{b}_0'(\boldsymbol{\omega}+\boldsymbol{\pi}_i) = \boldsymbol{P}_i\big(\boldsymbol{b}_0 - m_0\widetilde{\mathbf{M}}[:,0](\boldsymbol{\omega}+\boldsymbol{\pi}_i)\big) = \boldsymbol{b}_i - m_0(\boldsymbol{\omega}+\boldsymbol{\pi}_i)\boldsymbol{P}_i\big(\widetilde{\mathbf{M}}[:,0](\boldsymbol{\omega}+\boldsymbol{\pi}_i)\big)$$

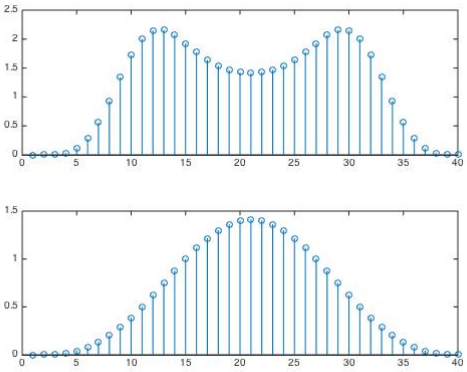

Figure 13: $m_0(\omega)$ and $\widetilde{m_0}(\omega)$

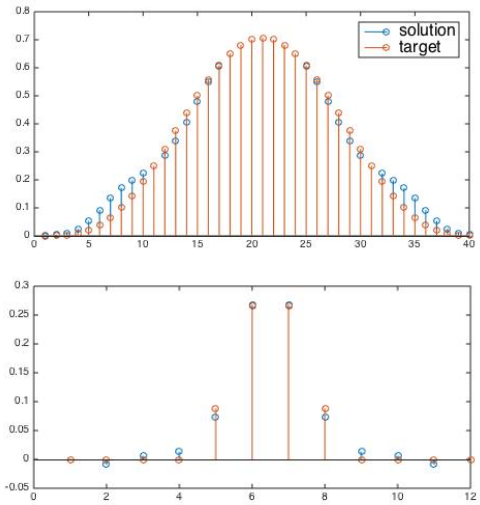

Figure 14: $\widehat{\widetilde{m_0}}$ vs. $\widetilde{m_0}$, top: frequency domain, bottom: time domain

and

$$\boldsymbol{P}_i\big(\widetilde{\mathbf{M}}[:,0](\boldsymbol{\omega}+\boldsymbol{\pi}_i)\big) = \begin{cases} \widetilde{\mathbf{M}}[:,0] = \overline{\widetilde{\mathbf{m}_0}}^{\mathcal{E}}, & i \text{ is even} \\ \overline{\widetilde{\mathbf{m}_0}}^{\mathcal{O}}, & i \text{ is odd} \end{cases}$$

Substitute the above expression of $\boldsymbol{P}_i\boldsymbol{b}_0'(\boldsymbol{\omega}+\boldsymbol{\pi}_i)$ in (40) and we have

$$\mathbf{0} = \boldsymbol{P}_{\widetilde{\mathbf{M}}}(\boldsymbol{I}_8 - \overline{\widetilde{\mathbf{m}_0}}^{\mathcal{E}} \otimes \overline{\mathbf{m}_0^{\mathcal{E}}} - \overline{\widetilde{\mathbf{m}_0}}^{\mathcal{O}} \otimes \overline{\mathbf{m}_0^{\mathcal{O}}}) \tag{41}$$

Therefore, by Lemma B.6, $\boldsymbol{P}_{\widetilde{\mathbf{M}}}$ is the projection of $span\{\overline{\mathbf{m}_0^{\mathcal{O}}}, \overline{\mathbf{m}_0^{\mathcal{E}}}\}$. This is equivalent to (28) and (29). Finally, since

$$6 = rank(\widetilde{\mathbf{M}}[:,-0]) \le rank(\widetilde{\mathbf{M}}[odd,-0]) + rank(\widetilde{\mathbf{M}}[even,-0]) \le (4-1)+(4-1),$$

$rank(\widetilde{\mathbf{M}}[odd,-0]) = rank(\widetilde{\mathbf{M}}[even,-0]) = 3$. □

C Supplementary Numerical Results

C.1 Numerical optimization of $\widetilde{m_0}(\boldsymbol{\omega})$ in 1D

To test whether numerical optimization is a practical way to solve (17) and (21), we experiment on m_0 and $\widetilde{m_0}$ of existing bi-orthogonal wavelets. We consider a pair of low frequency filters corresponding to bi-orthogonal scaling functions ϕ, $\tilde{\phi}$ with vanishing moments 3 and 5 respectively.

The 1D filters are shown in Fig.12. Suppose we know the decomposition filter, and we want to find the reconstruction filter by solving (21), such that the filter has support as concentrated as possible. Without loss of generality, (21) can be solved assuming that m_0 is real. It is not necessary that the corredponding $\widetilde{m_0}$ is also real, but in this testing case, m_0 and $\widetilde{m_0}$ are both real. Fig.13 shows the ground truth m_0 and $\widetilde{m_0}$ considered in this simulation.

Let $\widehat{\widetilde{m_0}}(\boldsymbol{\omega})$ be the approximation of $\widetilde{m_0}(\boldsymbol{\omega})$, which is solution of the following optimization problem

$$\min_{\mathbf{x}} \ \|\boldsymbol{D}\mathbf{x}\|^2 + \|\mathbf{x}\|^2, \quad s.t.\ \boldsymbol{A}\mathbf{x} = \mathbf{1} \tag{42}$$

where $\boldsymbol{A}$ in the constraint is the matrix generated from (17)

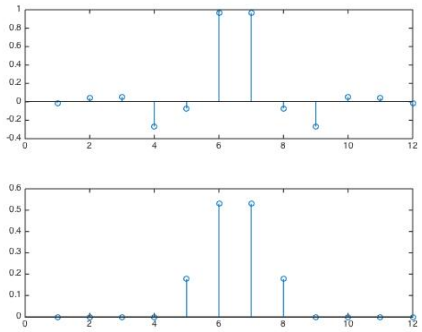

Figure 12: 1D filters, up: LoD, down: LoR

(in 1D, only a single shift of π appears in the condition, so each row of $\boldsymbol{A}$ has two non-zero entries). Figure 14 compares the solution of (42) and the ground truth. The support of the solution is slightly more spread out than the ground truth.

C.2 Numerical optimization of $\widetilde{m_0}(\boldsymbol{\omega})$ in 2D

In the 2D case, we use the pair of bi-orthogonal low-pass filters that are the tensor products of the 1D filters in Section C.1 as ground truth. We solve the 2D version of the optimization problem (42). Figure 15 shows the solution and compares it with the ground truth.

To make the support of $\widehat{\widetilde{m_0}}(\boldsymbol{\omega})$ better concentrate within the low frequency domain, we change the squared ℓ_2-norm penalty in (42) to a weighted version (corresponding to Modulation space) as follows,

$$\min_{\mathbf{x}} \ \|\boldsymbol{D}\mathbf{x}\|^2 + \lambda\|\mathbf{w}\circ\mathbf{x}\|^2, \quad s.t.\ \boldsymbol{A}\mathbf{x} = \mathbf{1} \tag{43}$$

where $\circ$ is Hadamard product and $\mathbf{w}$ is a weight vector. In particular, we choose $\forall\boldsymbol{\omega},\ \mathbf{w}(\boldsymbol{\omega}) = \|\boldsymbol{\omega}\|$. Fig.16 shows the solution of (43) with $\lambda = 600$.

Compared to (32) proposed to solve $\widetilde{m_0}(\boldsymbol{\omega})$, both optimization problems (42) and (43) in this simulation minimize total variation(TV) of $\widetilde{m_0}$ instead of $\widehat{\widetilde{m_0}}\cdot m_0$ and have an extra (weighted) ℓ_2 regularization term. Although (42) and (43) work better than (32) for tensor wavelet construction here, they do not provide better solutions in the construction of directional wavelets and cost more computation time.

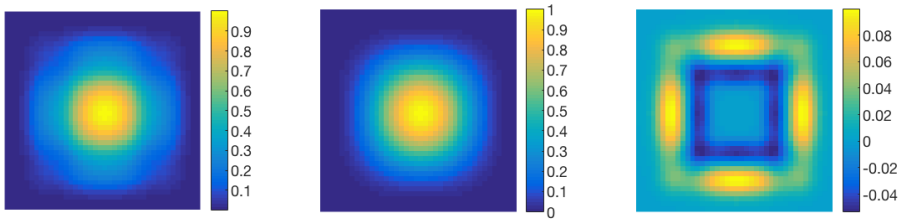

Figure 15: Left to right: solution of (42) in 2D, ground truth and their difference

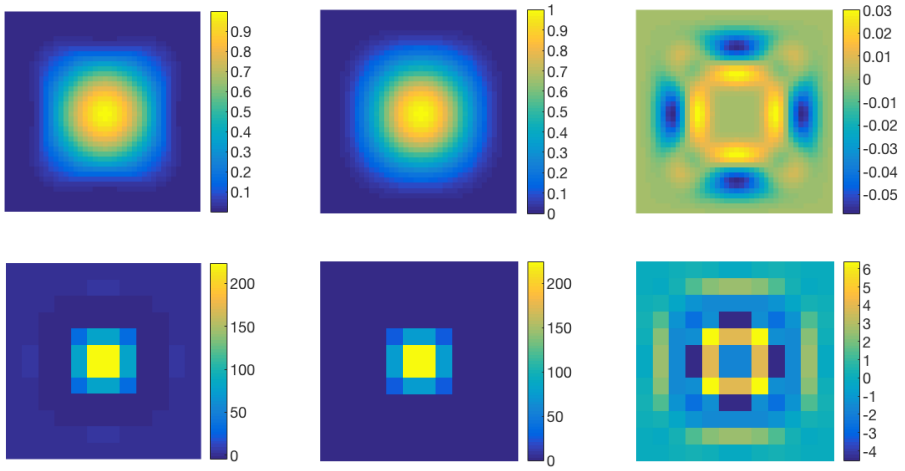

Figure 16: Left to right: solution of (43) ($\lambda = 600$), ground truth and their difference; Top: frequency domain, bottom: time domain.

References

[1] R. H. Bamberger and M. J. T. Smith, "A filter bank for the directional decomposition of images: theory and design," *IEEE Transactions on Signal Processing*, vol. 40, no. 4, pp. 882–893, Apr 1992.

[2] T. T. Nguyen and S. Oraintara, "Multiresolution direction filterbanks: theory, design, and applications," *IEEE Transactions on Signal Processing*, vol. 53, no. 10, pp. 3895–3905, Oct 2005.

[3] M. N. Do and M. Vetterli, "The contourlet transform: an efficient directional multiresolution image representation," *Image Processing, IEEE Transactions on*, vol. 14, no. 12, pp. 2091–2106, 2005.

[4] T. Sauer, "Shearlet multiresolution and multiple refinement." Kutyniok, Gitta (ed.) et al., Shearlets. Multiscale analysis for multivariate data. Boston, MA: Birkhäuser. Applied and Numerical Harmonic Analysis, 199-237 (2012)., 2012.

[5] G. Easley, D. Labate, and W.-Q. Lim, "Sparse directional image representations using the discrete shearlet transform," *Applied and Computational Harmonic Analysis*, vol. 25, no. 1, pp. 25–46, 2008.

[6] E. Candes, L. Demanet, D. Donoho, and L. Ying, "Fast discrete curvelet transforms," *Multiscale Modeling & Simulation*, vol. 5, no. 3, pp. 861–899, 2006.

[7] I. W. Selesnick, R. G. Baraniuk, and N. C. Kingsbury, "The dual-tree complex wavelet transform," *Signal Processing Magazine, IEEE*, vol. 22, no. 6, pp. 123–151, 2005.

[8] S. Durand, "M-band filtering and nonredundant directional wavelets," *Applied and Computational Harmonic Analysis*, vol. 22, no. 1, pp. 124 – 139, 2007.

[9] R. Yin, "Construction of orthonormal directional wavelets based on quincunx dilation subsampling," in *Sampling Theory and Applications (SampTA), 2015 International Conference on*, May 2015, pp. 292–296.

[10] A. Cohen and J.-M. Schlenker, "Compactly supported bidimensional wavelet bases with hexagonal symmetry," *Constructive approximation*, vol. 9, no. 2-3, pp. 209–236, 1993.

[11] A. Cohen, I. Daubechies, and J.-C. Feauveau, "Biorthogonal bases of compactly supported wavelets," *Communications on pure and applied mathematics*, vol. 45, no. 5, pp. 485–560, 1992.

[12] G. Kutyniok, W.-Q. Lim, and X. Zhuang, "Digital shearlet transforms," in *Shearlets*. Springer, 2012, pp. 239–282.